

# Mobility-aware Content Preference Learning in Decentralized Caching Networks

Yu Ye, *Student Member, IEEE*, Ming Xiao, *Senior Member, IEEE*, and Mikael Skoglund, *Fellow, IEEE*

**Abstract**—Due to the drastic increase of mobile traffic, wireless caching is proposed to serve repeated requests for content download. To determine the caching scheme for decentralized caching networks, the content preference learning problem based on mobility prediction is studied. We first formulate preference prediction as a decentralized regularized multi-task learning (DRMTL) problem without considering the mobility of mobile terminals (MTs). The problem is solved by a hybrid Jacobian and Gauss-Seidel proximal multi-block alternating direction method (ADMM) based algorithm, which is proven to conditionally converge to the optimal solution with a rate  $O(1/k)$ . Then we use the tool of *Markov renewal process* to predict the moving path and sojourn time for MTs, and integrate the mobility pattern with the DRMTL model by reweighting the training samples and introducing a transfer penalty in the objective. We solve the problem and prove that the developed algorithm has the same convergence property but with different conditions. Through simulation we show the convergence analysis on proposed algorithms. Our real trace driven experiments illustrate that the mobility-aware DRMTL model can provide a more accurate prediction on geography preference than DRMTL model. Besides, the hit ratio achieved by most popular proactive caching (MPC) policy with preference predicted by mobility-aware DRMTL outperforms the MPC with preference from DRMTL and random caching (RC) schemes.

**Index Terms**—Proactive caching; distributed machine learning; multi-task learning

## I. INTRODUCTION

As a promising technology for the fifth-generation (5G) wireless networks and beyond, *proactive caching* can alleviate the heavy traffic burden on backhaul links and reduce service delay, through proactively storing popular contents at base stations (BSs) and mobile terminals (MTs) [1]–[3]. With the limitation of storage memory, determining where and what to cache in content centric wireless networks becomes one of the main challenges in the design of proactive caching schemes. Among the various factors affecting the wireless caching design, involving the mobility of MTs and learning content preference are two critical challenges, which have attracted more and more research interest recently.

### A. background

Current investigation on mobility aware wireless caching mainly includes two aspects: studying the impact of MT mobility on caching schemes [4]–[7], and optimizing the wireless caching schemes based on the mobility information of MTs

[8]–[17]. A general framework on mobility-aware caching in content-centric wireless networks is presented in [4]. In [5], groups of mobile devices collaborating to exchange contents via BS assisted D2D communications, the deterministic and random caching strategies at MTs are analyzed, and it is shown that the latter may be more realistic in networks with MT mobility. The effect of user mobility on the coverage probability of D2D networks with distributed caching is studied in [6].

Meanwhile, most of the recent results optimize caching schemes by considering mobility over different metrics. In [8], [9], with the goal of minimizing the probability of using macro BSs for content delivery, mobility-aware storage allocation schemes for wireless caching in a two-tier heterogeneous network (HetNet) is studied. In [10], the proactive caching problem is investigated for cloud radio access networks (CRANs), where the caching scheme for remote radio heads and the baseband units (BBUs) is optimized to maximize the effective capacity. The mobility patterns of MTs are predicted through echo state networks (ESNs) at BBUs. In [11], the inter-contact time between MTs is considered, and a mobility-aware caching strategy is developed to maximize the percentage of requested data delivered via D2D links. In [15], a novel mobility-aware coded probabilistic caching scheme is proposed for mobile edge computing (MEC) enabled small cell networks (SCNs) to maximize the throughput. The optimization of mobility-aware caching schemes for maximizing the hit ratio is studied in [16] and [17]. The contact time of MTs is evaluated in [16] through modeling MT mobility as a *Markov renewal process*, and the proactive caching design at BSs and MTs is optimized to maximize the hit ratio. While a peer-to-peer connectivity model is used to obtain the mobility pattern of users and mobility-aware caching placement for maximizing the cache hit ratio is investigated in [17].

For most references above, the content preference of MTs is assumed to be known. This however is not realistic. Since the preference of contents, which varies with time and location, plays an important role to the performance of proactive caching scheme, it should be continuously learned and updated. According to [18], content preference for a group of users follows a Zipf-like distribution. Hence learning methods are proposed to obtain the content preference from request history and the context of MTs [10], [12], [19]–[23]. In [10], the ESNs are also used at BBUs to predict MT content request distribution from the context information of MTs. But the implementation of the proposed method is complex since the system has to generate one ESN for each MT. Reference [12] provides a user interest prediction model, which combines the social proximity and dynamic

Yu Ye, Ming Xiao and Mikael Skoglund are with the School of Electrical Engineering and Computer Science, Royal Institute of Technology (KTH), Stockholm, Sweden (email: yu9@kth.se, mingx@kth.se, skoglund@kth.se).

content popularity. In [19], content popularity is unknown and estimation uses instantaneous demands from users within a specified time interval. To reduce learning time, a transfer learning-based approach is proposed, where extra source domain samples are provided for estimation. The authors in [20] construct an extreme learning machine (ELM) to estimate popularity. In [24], content preference is learned by multi-armed bandit method incorporated with the content caching and sharing process. The algorithm that learns context-specific content popularity online by regularly observing the context information of connected users is presented in [21]. Further in [23], an offline user preference learning approach is studied.

### B. motivation

To reduce traffic, wireless caching seeks to store the common popular contents at the edge of the network. The geographic caching scheme is studied in [25]. Since the MTs may have heterogeneous preference [26], the mobility of MTs will cause the content preference in different locations to vary with time. This is presented in Fig. 1, where the geography preference observed by agent 4 is determined by the movement of MTs. Thus to achieve mobility-aware content placement, wireless caching networks should learn the geography preference incorporating the mobility patterns of MTs rather than only learn the individual MT preference [19]–[23].

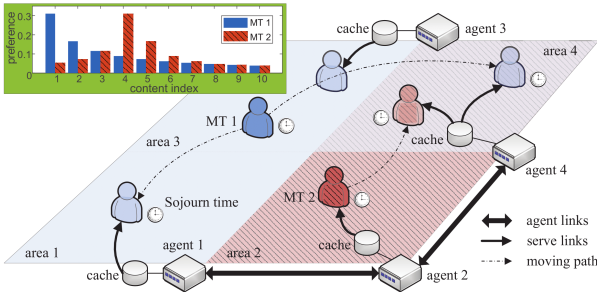


Fig. 1. The system model of mobility-aware MTL proactive caching in decentralized content centric wireless networks.

Since the data used to learn the user preference is first observed by local agents, in order to implement the learning in a central manner, tremendous amounts of data need to be transmitted. This can cause heavy communication load. Furthermore, due to the constraint of data privacy and security, distributed learning method is preferred on predicting the geography preference in decentralized networks. Although distributed caching is studied in [27]–[29], none of these references provides machine learning based approaches for predicting the mobility-aware geography preference. Considering cooperative caching [30] and transmission [31], the proactive caching schemes in different spatial areas should be optimized jointly. Hence the agent in Fig. 1 should be aware of what the preference is like at its neighboring areas. To achieve this requirement, we take advantage of the regularized multi-task learning (RMTL) method [32] and extend it to a decentralized setting. This is because the geography preference for adjacent area is correlated due to the movement of MTs.

In what follows, we shall study how to predict the content preference in geography aspects with distributed learning methods and mobility prediction. The main contributions of this paper are listed as follows.

- We model geography preference prediction in distributed caching networks as a decentralized RMTL (DRMTL) problem, which is solved by proposed hybrid Jacobian and Gauss-Seidel proximal multi-block alternating direction method (ADMM).
- We model the MT moving pattern through a *Markov renewal process* to predict the moving paths and sojourn time. Then we integrate the mobility into the DRMTL model by reweighting examples and introducing a transfer penalty in order to control the information exchanged across adjacent agents. The problem solution is provided.
- We generalize the DRMTL problem as majorized multi-block convex optimization with coupled objective functions. We show that the mobility-aware DRMTL model is consistent with the DRMTL problem, and prove that proposed solutions converge to optimum with  $O(1/k)$  rate when algorithm parameters meet specific conditions.
- By simulation, we verify the convergence of proposed algorithms. With experiments on real trajectory dataset, we show that, compared with the DRMTL model, the mobility-aware DRMTL model can provide a more accurate prediction on geographic preference, with which the most popular proactive caching (MPC) scheme can achieve a better hit ratio than MPC with preference from DRMTL and random caching (RC) scheme.

The rest of this paper is organized as follows. We present the system model of preference prediction and formulate it as a DRMTL problem in Section II. Then hybrid Jacobian and Gauss-Seidel proximal ADMM based algorithm (Algorithm 1) is provided, together with its convergence analysis. In section III the mobility prediction model is first presented, followed by the formulation of mobility-aware DRMTL problem, as well as the proposed Algorithm 2 and convergence proof. Numerical results are given in Section IV to evaluate the convergence and preference prediction performance of the proposed approaches. Finally, we draw conclusions in Section V.

## II. SYSTEM MODEL AND DECENTRALIZED CONTENT PREFERENCE LEARNING

The system model for content preference prediction is shown in Fig. 1. Each spatial area is controlled by one agent, and there is no overlap for adjacent areas. In the DRMTL setup, each task runs at one agent. Hence for simplicity, we use the agent to stand for the corresponding area and task. We define the decentralized network by an undirected graph  $\mathcal{G}(\mathcal{V}, \mathcal{E})$ , where  $\mathcal{V}$  includes all agents and  $\mathcal{E}$  includes all connection among them. We denote  $\mathcal{V}_i \subset \mathcal{V}$  as the neighboring agents for  $i \in \mathcal{V}$ , where  $(i, j) \in \mathcal{E}$  if  $j \in \mathcal{V}_i$ . The MTs located within areas  $\mathcal{V}$  are  $\mathcal{M} = \{1, \dots, M\}$ , and the interested contents for MTs are  $\mathcal{F} = \{1, \dots, F\}$ , where  $F \in \mathbb{N}_+$ . Following [26] we categorize MTs into  $K$  groups according to their content preference, denoted by the set  $\mathcal{K} = \{1, \dots, K\}$ . The content preference for group  $i \in \mathcal{K}$  is  $P_i$ . Without loss of

generality, we assume MTs requesting contents with fixed rate  $R_f$ . For each request from an MT in group  $i \in \mathcal{K}$ , it follows distribution  $P_i$ . Moreover the request can only be served by the agent where the MT located. In order to determine the content placement in proactive caching for future time window  $[0, t_d]$ , each agent needs to predict the content preference from the observed request history  $\mathcal{D}_i = \{x_{i,l}, y_{i,l} | l = 1, \dots, b_i\}$  before time 0 at its covered area. Then each agent determines what to cache at time 0. During  $[0, t_d]$ , MTs may move around within agents. Besides we assume that dataset cannot be shared among neighboring agents.

In what follows, we will first formulate the decentralized content preference learning model based on DRMTL.

### A. Problem Formulation

Considering a decentralized network  $\mathcal{G}(\mathcal{V}, \mathcal{E})$ , for simplicity, we denote  $|\mathcal{V}| = N$ . We formulate preference prediction by the DRMTL model, where MTs are assumed to be stationary and agents cooperatively solve the following problem

$$\min_{\mathbf{w}_i} \sum_{i \in \mathcal{V}} f_i(\mathbf{w}_i), \quad (1)$$

where  $\mathbf{w}_i = \mathbf{w}_0 + \hat{\mathbf{w}}_i$  and  $f_i(\cdot)$  is the local loss function of task  $i$ .  $\mathbf{w}_0$  is common among agents while  $\hat{\mathbf{w}}_i$  is the specific weight for tasks. The main reason of using DRMTL in content preference learning is that  $\mathbf{w}_0$  can capture basis content preference across the adjacent geography areas, while  $\mathbf{w}_i$  represents the variance of content preference of task  $i$ . Similar to [32], the model parameters  $\mathbf{w}_0$  and  $\hat{\mathbf{w}}_i$  can be learned at the central processor, if it has access to all datasets. However, the data collected by different agents are geo-distributed. Therefore we consider the RMTL in decentralized networks. In the decentralized setting, if the parameters are learned separately by agents, a common  $\mathbf{w}_0$  cannot be guaranteed. To solve this problem, we exploit the alternating direction method of multipliers (ADMM) to ensure all agents agree with the same basis by introducing basis weights  $\check{\mathbf{w}}_i$  at each agent and the consensus constraints  $\check{\mathbf{w}}_i = \check{\mathbf{w}}_j, \forall (i, j) \in \mathcal{E}$ . The problem is formulated as

$$\min_{\check{\mathbf{W}}, \hat{\mathbf{W}}} \sum_{i \in \mathcal{V}} \left( f_i(\check{\mathbf{w}}_i, \hat{\mathbf{w}}_i, \mathcal{D}_i) + \frac{\mu_1}{2} \|\check{\mathbf{w}}_i\|^2 + \frac{\mu_2}{2} \|\hat{\mathbf{w}}_i\|^2 \right), \quad (\text{P1})$$

s.t.  $\mathbf{A}\check{\mathbf{W}} = \mathbf{0}$ .

where  $\check{\mathbf{W}} = [\check{\mathbf{w}}_1, \dots, \check{\mathbf{w}}_N]$ ,  $\hat{\mathbf{W}} = [\hat{\mathbf{w}}_1, \dots, \hat{\mathbf{w}}_N]$ ,  $\mathbf{A} = [A_1, \dots, A_N]$ , and  $\mathbf{A}$  can be derived by  $\mathcal{G}$ .  $\mathcal{D}_i$  is the dataset at agent  $i$ , where  $x_{i,l} \in \mathbb{R}_+^n$  is the feature of MT while  $y_{i,l} \in \mathbb{R}_+^v$  is the associated request history. Without loss of generality, we assume  $\check{\mathbf{w}}_i, \hat{\mathbf{w}}_i \in \mathbb{R}^n$ , and denote  $f_i(\check{\mathbf{w}}_i, \hat{\mathbf{w}}_i, \mathcal{D}_i) = \frac{1}{b_i} \sum_{l=1}^{b_i} \ell(\check{\mathbf{w}}_i, \hat{\mathbf{w}}_i, x_{i,l}, y_{i,l})$  as the local function, where  $\ell(\cdot) : \mathbb{R}^n \rightarrow \mathbb{R}^v$  is the loss function. The predicted preference during  $[0, t_d]$  at agent  $i$  can be obtained by  $y_{i,0} = f_i(\check{\mathbf{w}}_i, \hat{\mathbf{w}}_i, x_{i,0})$ , where  $x_{i,0}$  is the input at time 0. For convenience we denote  $f_i(\check{\mathbf{w}}_i, \hat{\mathbf{w}}_i, \mathcal{D}_i)$  as  $f_i(\check{\mathbf{w}}_i, \hat{\mathbf{w}}_i)$ .

Problem (P1) can be solved with the proximal ADMM method [33]. The augmented Lagrange function is given by

$$\mathcal{L}_\rho^1(\check{\mathbf{W}}, \hat{\mathbf{W}}, \lambda) = \sum_i \left( f_i(\check{\mathbf{w}}_i, \hat{\mathbf{w}}_i) + \frac{\mu_1}{2} \|\check{\mathbf{w}}_i\|^2 + \frac{\mu_2}{2} \|\hat{\mathbf{w}}_i\|^2 + \lambda^T \mathbf{A}\check{\mathbf{W}} + \frac{\rho}{2} \|\mathbf{A}\check{\mathbf{W}}\|^2 \right), \quad (2)$$

---

### Algorithm 1:

---

- 1: **initialize:** set  $\{\check{\mathbf{w}}_i^0, \hat{\mathbf{w}}_i^0 | i \in \mathcal{V}\}$  randomly and  $\lambda^0 = \mathbf{0}$
  - 2: **for**  $k = 0, 1, \dots$  **do**
  - 3:   **agents**  $i = 1$  **to**  $N$ :
  - 4:   update  $\check{\mathbf{w}}_i^{k+1}$  with (3) *in parallel* ;
  - 5:   communicate  $\check{\mathbf{w}}_i^{k+1}$  with neighboring agents and update  $\lambda^{k+1}$  with (4).
  - 6:   **agents**  $i = 1$  **to**  $N$ :
  - 7:   update  $\hat{\mathbf{w}}_i^{k+1}$  with (5) *in parallel*;
  - 8: **end for**
- 

where  $\lambda$  is a Lagrange multiplier and  $\rho (> 0)$  is a constant parameter. The constraint matrix satisfies  $A_i^T A_i = d_i I$ , where  $I$  is an identity matrix,  $d_i = |\mathcal{V}_i|$  is the degree of agent  $i$ , and  $A_i^T A_j = \mathbf{0}$  if  $(i, j) \notin \mathcal{E}$ . By defining the set  $\check{\mathbf{W}}_{-i}^k = [\check{\mathbf{w}}_1, \dots, \check{\mathbf{w}}_{i-1}, \check{\mathbf{w}}_{i+1}, \dots, \check{\mathbf{w}}_N]$ , the update of hybrid Jacobi and Gauss-Seidel type ADMM follows

$$\check{\mathbf{w}}_i^{k+1} := \arg \min \mathcal{L}_\rho(\check{\mathbf{w}}_i, \hat{\mathbf{w}}_i^k, \check{\mathbf{W}}_{-i}^k, \lambda^k) + \frac{1}{2} \|\check{\mathbf{w}}_i - \check{\mathbf{w}}_i^k\|_{P_i}^2, \quad (3)$$

$$\lambda^{k+1} := \lambda^k + \gamma \rho \mathbf{A} \check{\mathbf{W}}^{k+1}, \quad (4)$$

$$\hat{\mathbf{w}}_i^{k+1} := \arg \min \mathcal{L}_\rho(\hat{\mathbf{w}}_i, \check{\mathbf{w}}_i^{k+1}) + \frac{1}{2} \|\hat{\mathbf{w}}_i - \hat{\mathbf{w}}_i^k\|_{Q_i}^2, \quad (5)$$

where  $k$  is the iteration number. Then we conclude Algorithm 1 to solve (P1). In Algorithm 1, the values of  $\check{\mathbf{w}}_i$  and  $\hat{\mathbf{w}}_i$  are randomly initialized. In iteration  $k$ ,  $\check{\mathbf{w}}_i^{k+1}$  is firstly updated at each agent in parallel and then communicated to agent  $j$  where  $(i, j) \in \mathcal{E}$ . The Lagrange  $\lambda$  regarding to all connections is then updated with  $\check{\mathbf{w}}_i^{k+1}$ . At the end of iteration  $k$ , the local weights  $\hat{\mathbf{w}}_i$  are optimized separately across agents. It is worth noting that Algorithm 1 is synchronous ADMM since the clock  $k$  is kept unique among agents.

### B. Convergence analysis

In what follows, we will analyze the convergence properties of the proposed Algorithm 1. It is worth noting that (P1) is a majorized multi-block ADMM with coupled objective functions, which is preliminarily studied in [34]–[36]. Our proof is different from that of [36], where a hybrid Jacobian and Gauss-Seidel proximal block coordinate update (BCU) method is presented to solve a linearly constrained multi-block structured problem with a quadratic term in objective. The similar type algorithm is also provided in [37] to solve a multi-convex problem. We start with the following two assumptions.

**Assumption 1.** *The undirected graph  $\mathcal{G}$  is connected.*

The Assumption 1 ensures that the consensus for  $\check{\mathbf{w}}_i$  can be guaranteed in Algorithm 1. Defining  $\mathbf{z}_i = [\check{\mathbf{w}}_i, \hat{\mathbf{w}}_i]$ , we present the assumption on the loss function  $f_i$ .

**Assumption 2.** *The local loss function  $f_i$  is differentiable and jointly convex over  $\check{\mathbf{w}}_i$  and  $\hat{\mathbf{w}}_i$ . The gradient of  $f_i$  is Lipschitz continuous*

$$\|\nabla f_i(\mathbf{z}_i^1) - \nabla f_i(\mathbf{z}_i^2)\| \leq C_i \|\mathbf{z}_i^1 - \mathbf{z}_i^2\|, \quad \forall \mathbf{z}_i^1, \mathbf{z}_i^2 \in \mathbb{R}^n \times \mathbb{R}^n, \quad (6)$$

where  $C_i$  is the Lipschitz constant.

Denoting  $g(\check{\mathbf{w}}_i) = \frac{\mu_i}{2} \|\check{\mathbf{w}}_i\|^2$  and  $h(\hat{\mathbf{w}}_i) = \frac{\mu_i}{2} \|\hat{\mathbf{w}}_i\|^2$ , further with Assumption 2, we obtain the following useful inequality for loss function  $f_i$ .

**Lemma 1.** For any  $\mathbf{z}_i^1, \mathbf{z}_i^2, \mathbf{z}_i^3 \in \mathbb{R}^n \times \mathbb{R}^n$ ,

$$f_i(\mathbf{z}_i^2) \leq f_i(\mathbf{z}_i^1) + (\mathbf{z}_i^2 - \mathbf{z}_i^1)^T \nabla f_i(\mathbf{z}_i^3) + \frac{C_i}{2} \|\mathbf{z}_i^2 - \mathbf{z}_i^3\|^2. \quad (7)$$

With the convexity of  $g(\check{\mathbf{w}}_i)$  and the strong convexity of  $h(\hat{\mathbf{w}}_i)$  with constant  $m(> 0)$ , we have

$$(\check{\mathbf{w}}_i^1 - \check{\mathbf{w}}_i^2)^T g'(\check{\mathbf{w}}_i^2) \leq g'(\check{\mathbf{w}}_i^1) - g'(\check{\mathbf{w}}_i^2), \quad (8)$$

$$(\hat{\mathbf{w}}_i^1 - \hat{\mathbf{w}}_i^2)^T h'(\hat{\mathbf{w}}_i^2) + \frac{m}{2} \|\hat{\mathbf{w}}_i^1 - \hat{\mathbf{w}}_i^2\|^2 \leq h'(\hat{\mathbf{w}}_i^1) - h'(\hat{\mathbf{w}}_i^2). \quad (9)$$

*Proof.* Following Fact 2 in [38], (7) can be shown directly. (8) holds because of the convexity of  $g(\cdot)$ . Since  $m = 2$  can make (9) satisfied,  $h(\cdot)$  is strongly convex.  $\square$

With Assumption 1 and Lemma 1, we then present the global convergence of Algorithm 1. To simplify the notation, we denote

$$\mathbf{G}_1 := \text{blkdiag}(\rho A_1^T A_1 + P_1, \dots, \rho A_N^T A_N + P_N), \quad (10)$$

$$\mathbf{G}_2 := \text{blkdiag}(Q_1, \dots, Q_N), \quad (11)$$

$$\mathbf{G}_3 := \text{blkdiag}\left(\frac{C_1}{m}(C_1 + m), \dots, \frac{C_N}{m}(C_N + m)\right), \quad (12)$$

$$\mathbf{G} := \text{blkdiag}\left(\mathbf{G}_1, \mathbf{G}_2, \frac{1}{\gamma\rho} I\right), \quad (13)$$

$$\mathbf{M} := \begin{bmatrix} \mathbf{G}_1 & \mathbf{0} & \frac{1}{\gamma} \mathbf{A}^T \\ \mathbf{0} & \mathbf{G}_2 - \mathbf{G}_3 & \mathbf{0} \\ \frac{1}{\gamma} \mathbf{A} & \mathbf{0} & \frac{2-\gamma}{\gamma^2\rho} I \end{bmatrix}, \quad (14)$$

where  $\text{blkdiag}(\cdot)$  stands for the block-diagonal matrix. Denote  $\{\mathbf{u}^{k+1} = [\check{\mathbf{W}}^{(k+1)T}, \hat{\mathbf{W}}^{(k+1)T}, \lambda^{(k+1)T}]^T, k \geq 1\}$  as the sequence generated by Algorithm 1 after the  $k$ -th iteration. Our analysis focuses on bounding the error  $\|\mathbf{u}^k - \mathbf{u}^*\|_{\mathbf{G}}^2$  and showing that it decreases with iterations, where  $\mathbf{u}^*$  is the optimal solution for (P1).

**Lemma 2.** For  $k \geq 1$ , the sequence  $\mathbf{u}^k$  satisfies

$$\|\mathbf{u}^k - \mathbf{u}^*\|_{\mathbf{G}}^2 - \|\mathbf{u}^{k+1} - \mathbf{u}^*\|_{\mathbf{G}}^2 \geq \|\mathbf{u}^k - \mathbf{u}^{k+1}\|_{\mathbf{M}}^2, \quad (15)$$

where

$$\begin{aligned} \|\mathbf{u}^k - \mathbf{u}^{k+1}\|_{\mathbf{M}}^2 &= \|\check{\mathbf{W}}^k - \check{\mathbf{W}}^{k+1}\|_{\mathbf{G}_1}^2 + \|\hat{\mathbf{W}}^k - \hat{\mathbf{W}}^{k+1}\|_{\mathbf{G}_2 - \mathbf{G}_3}^2 + \\ &\frac{2-\gamma}{\gamma^2\rho} \|\lambda^k - \lambda^{k+1}\|^2 + \frac{2}{\gamma} (\lambda^k - \lambda^{k+1})^T \mathbf{A} (\check{\mathbf{W}}^k - \check{\mathbf{W}}^{k+1}). \end{aligned} \quad (16)$$

*Proof.* See the Appendix A.  $\square$

If matrix  $\mathbf{M}$  is positive definite, then there exists some  $\eta > 0$  such that

$$\|\mathbf{u}^k - \mathbf{u}^*\|_{\mathbf{G}}^2 - \|\mathbf{u}^{k+1} - \mathbf{u}^*\|_{\mathbf{G}}^2 \geq \|\mathbf{u}^k - \mathbf{u}^{k+1}\|_{\mathbf{M}}^2 \geq \eta \|\mathbf{u}^k - \mathbf{u}^{k+1}\|^2. \quad (17)$$

(17) shows that with increasing iteration  $k$ , error  $\|\mathbf{u}^k - \mathbf{u}^*\|_{\mathbf{G}}^2$  is monotonically non-increasing and thus converging, and  $\|\mathbf{u}^k - \mathbf{u}^{k+1}\| \rightarrow 0$ . Then from the standard analysis for contraction

methods [39],  $\|\mathbf{u}^k - \mathbf{u}^*\|_{\mathbf{G}}^2 \rightarrow 0$  can be obtained immediately. In the following, we provide the conditions that guarantee the global convergence of Algorithm 1. For convenience we adopt *Standard Proximal* as  $P_i = \tau_i I$  and  $Q_i = \zeta_i I$ , where  $\tau_i, \zeta_i \in \mathbb{R}_+$ .

**Theorem 1.** (Convergence of Algorithm 1) If there exist  $0 < \epsilon_i < 1$  and  $0 < \gamma < 2$  such that  $\rho$ ,  $\tau_i$  and  $\zeta_i$  satisfy the following conditions:

$$\tau_i > \rho \left( \frac{1}{\epsilon_i} - 1 \right) d_i, \quad \zeta_i > \frac{C_i}{m} (C_i + m), \quad \sum_i \epsilon_i < 2 - \gamma, \quad (18)$$

then the sequence  $\mathbf{u}^k$  generated by Algorithm 1 converges to the global optimal solution  $\mathbf{u}^*$  of Problem (P1).

*Proof.* See the Appendix B.  $\square$

**Proposition 1.** By letting  $\epsilon_i < \frac{2-\gamma}{N}$ , condition (18) reduces to

$$\tau_i > \rho \left( \frac{N}{2-\gamma} - 1 \right) d_i, \quad \zeta_i > \frac{C_i}{m} (C_i + m). \quad (19)$$

*Proof.* The results can be straightly obtained from the proof of Theorem 1.  $\square$

Next we shall investigate the convergence rate of Algorithm 1. Here, we define

$$\mathbf{G}_1^\dagger := \mathbf{G}_1 - \rho \mathbf{A}^T \mathbf{A}, \quad (20)$$

and denote  $\mathbf{F}(\mathbf{Z}) = \sum_i F_i(\mathbf{z}_i) = \sum_i (f_i(\check{\mathbf{w}}_i, \hat{\mathbf{w}}_i) + g(\check{\mathbf{w}}_i) + h(\hat{\mathbf{w}}_i))$  with  $\mathbf{Z} = [\check{\mathbf{W}}, \hat{\mathbf{W}}]$ .

**Corollary 1.** (Convergence rate of Algorithm 1) If  $\mathbf{G}_1^\dagger > 0$ ,  $\mathbf{G}_2 > \mathbf{G}_3$ ,  $0 < \gamma < 2$  and  $\lambda^0 = \mathbf{0}$ , then we have

$$\mathbf{F}(\bar{\mathbf{Z}}^k) - \mathbf{F}(\mathbf{Z}^*) \leq \frac{1}{2k} \left( \|\check{\mathbf{W}}^0 - \check{\mathbf{W}}^*\|_{\mathbf{G}_1^\dagger}^2 + \|\hat{\mathbf{W}}^0 - \hat{\mathbf{W}}^*\|_{\mathbf{G}_2}^2 \right), \quad (21)$$

where  $\bar{\mathbf{Z}}^k = \frac{1}{k} \sum_{i=1}^k \mathbf{Z}^i$ .

*Proof.* See the Appendix C.  $\square$

Corollary 1 demonstrates that Algorithm 1 can guarantee a  $O(1/k)$  convergence rate in average.

**Proposition 2.** Since  $\|A_i^T A_j\| \leq \sqrt{n}$  ( $i, j \in \mathcal{V}, i \neq j$ ), to meet the requirements in Theorem 1 and Corollary 1,  $\zeta_i$  should satisfy (19) while  $\tau_i$  follows

$$\tau_i > \max \left\{ \rho d_i + 4(N-1)\rho\sqrt{n}, \rho \left( \frac{N}{2-\gamma} - 1 \right) d_i \right\}. \quad (22)$$

*Proof.* See the Appendix D.  $\square$

When  $Q_i$  adopts the *Standard Proximal* form, the requirement for  $\zeta_i$  in Theorem 1 and Corollary 1 is unique. But as for  $\tau_i$ , the conditions become different as summarized in Proposition 2. From (22) we can conclude that  $\tau_i$  is proportional to the number of agents  $N$ . For a larger decentralized network, the larger  $\tau_i$  is required for all agents. Moreover,  $\tau_i$  is also proportional to  $d_i$ , the degree of agent  $i$ . This is natural since the updated  $\check{\mathbf{w}}_i$  of task  $i$  with more connections affects the updating process of more agents. Hence to ensure the convergence, the step size should be reduced at agent  $i$ .

### III. MOBILITY-AWARE CONTENT PREFERENCE PREDICTION

In this section, we first introduce the mobility prediction model based on the tool of *Markov renewal processes* [16], [40] in a decentralized setting. Then by adopting the adaptive learning model, the predicted mobility pattern is integrated in DRMTL model. For the sake of secrecy, sharing the mobility information of MTs directly among agents is not allowed.

#### A. Mobility Prediction Model

The wireless user-mobility prediction has been extensively studied in [41]–[43]. Here we only focus on predicting the sojourn time for MTs. We consider the moving pattern for MTs  $\mathcal{M} = \{1, \dots, M\}$  located within  $\mathcal{V}$ . According to [16], we model MT  $m$  mobility as  $\{(S_{m,l}, T_{m,l}) : l \geq 0\}$ , to predict the moving path and the sojourn time within  $\mathcal{V}$  for a future time window  $[0, t_d]$ , where  $T_{m,l}$  is the time instant of the  $l$ -th transition ( $T_{m,0} = 0$ ), and  $S_{m,l} \in \mathcal{V}$  is the state at the  $l$ -th transition. The initial state for MT  $m$  is supposed to be  $S_{m,0}$ , and the time that MT  $m$  has stayed at  $S_{m,0}$  before time 0 is  $t_{m,0}$ . In the decentralized setting, agent  $i$  can only predict the movement of MTs  $\mathcal{M}_i$  to its neighbor agents  $j \in \mathcal{V}_i$ , where  $\mathcal{M}_i \subset \mathcal{M}$ ,  $\mathcal{M}_i \cap \mathcal{M}_j = \emptyset$ ,  $i, j \in \mathcal{V}$ ,  $i \neq j$  and  $\cup_{i \in \mathcal{V}} \mathcal{M}_i = \mathcal{M}$ . Considering MT  $m$  located at agent  $i$  where  $S_{m,0} = i$ , the transition probability of the embedded Markov chain is denoted as  $\mathbb{P}^{m,i} \in \mathbb{R}_+^{N \times N}$ , which is a row stochastic matrix and  $\mathbb{P}_{i,j}^{m,i} = 0$  if  $j \notin \mathcal{V}_i$ . Denote  $\Psi_{m,i}(x)$  as the probability mass function (pmf) of the sojourn time for MT  $m$  staying within agent  $i$ . We define the moving path set for MT  $m$  at agent  $i$  within time  $[0, t_d]$  as  $\mathcal{S}_m := \{S_{m,1}, \dots, S_{m,|\mathcal{S}_m|}\} (1 \leq |\mathcal{S}_m| \leq d_i)$  with initial state  $S_{m,j,0} = S_{m,0}$  for any path  $j (1 \leq j \leq |\mathcal{S}_m|)$ , where the  $j$ -th path is  $S_{m,j} := [S_{m,0}, \dots, S_{m,j,|\mathcal{S}_m,j|}]$ . Since MT  $m$  stays at area  $i$  for time  $T_{m,0}$ , the 1-st transition for all paths in  $\mathcal{S}_m$  is predicted to occur at time instant

$$T_{m,1} = \sum_{x=T_{m,0}}^{\infty} x \Psi_{m,i}(x). \quad (23)$$

Specially, we adopt the average sojourn time to predict the transition. Hence if  $T_{m,1} \geq t_d$ , we have  $|\mathcal{S}_m| = 1$  and  $S_{m,1} = i$  with path probability  $\Pr(S_{m,1}) = 1$ , otherwise  $|\mathcal{S}_m| = d_i$  and  $S_{m,j} := [i, S_{m,j,1}]$  where  $S_{m,j,1} \in \mathcal{V}_i$  with path probability

$$\Pr(S_{m,j}) = \mathbb{P}_{i, S_{m,j,1}}^{m,i}, \quad 1 \leq j \leq d_i. \quad (24)$$

Then for agent  $i$  and MT  $m \in \mathcal{M}_i$ , we can derive the predicted residence time to agent  $j$  as

$$r_{m,i \rightarrow j} = [t_d - T_{m,1}]_+ \mathbb{P}_{i,j}^{m,i}, \quad j \in \mathcal{V}_i, \quad (25)$$

where  $[a]_+ = a$  if  $a > 0$  otherwise 0. The prediction accuracy of mobility patterns for our provided model will be analyzed in Section V.

#### B. Mobility-Aware Preference Prediction

Inspired by the adaptive learning method [44] and distributed MTL model in [45], we modify the DRMTL in (P1) to the following problem (P2), which integrates the predicted mobility pattern of MTs,

$$\begin{aligned} \min_{\tilde{\mathbf{w}}, \hat{\mathbf{w}}} \quad & \sum_{i \in \mathcal{V}} \left( \tilde{f}_i(\tilde{\mathbf{w}}_i, \hat{\mathbf{w}}_i) + \frac{\mu_1}{2} \|\tilde{\mathbf{w}}_i\|^2 + \frac{\mu_2}{2} \|\hat{\mathbf{w}}_i\|^2 + \right. \\ & \left. \frac{\mu_3}{2} \sum_{j \in \mathcal{V}_i} c_{j,i} \|\mathbf{w}_{j,i}^{\text{loc}} - (\tilde{\mathbf{w}}_i + \hat{\mathbf{w}}_i)\|^2 \right), \\ \text{s.t.} \quad & \mathbf{A}\tilde{\mathbf{W}} = \mathbf{0}, \\ & \mathbf{w}_{i,j}^{\text{loc}} = \arg \min_{\mathbf{w}} \tilde{f}_{i \rightarrow j}(\mathbf{w}) + \frac{\mu_{12}}{2} \|\mathbf{w}\|^2, \quad i \in \mathcal{V}, j \in \mathcal{V}_i, \end{aligned} \quad (\text{P2})$$

where

$$\tilde{f}_i(\tilde{\mathbf{w}}_i, \hat{\mathbf{w}}_i) = \frac{1}{b_i} \sum_{l=1}^{b_i} \phi_{i,l} \ell(\tilde{\mathbf{w}}_i, \hat{\mathbf{w}}_i, x_{i,l}, y_{i,l}), \quad (26)$$

$$\tilde{f}_{i \rightarrow j}(\mathbf{w}) = \frac{1}{b_i} \sum_{l=1}^{b_i} \phi_{i \rightarrow j, l} \ell(\mathbf{w}, x_{i,l}, y_{i,l}). \quad (27)$$

In (P2),  $\mathbf{w}_{i,j}^{\text{loc}}$  denotes the weights transferred from agent  $i$  to  $j$ . It contains the information for the leaving crowds of  $\mathcal{M}_i$  to  $j$ . The adaptive parameters  $\phi_{i,l}, \phi_{i \rightarrow j, l} \in (0, 1]$  are chosen by agent  $i$  according to the predicted moving pattern of MTs  $\mathcal{M}_i$ . Hence (26) and (27) can be seen as a reweighting of the examples as [44].  $\{c_{i,j}\}$  are the non-negative task combiners, which control the similarity of transformed weights and local ones of neighboring agents [45].  $c_{i,j}$  is generated at agent  $i$  according to the leaving crowd to agent  $j$ . To present the settings of  $\phi_{i,l}, \phi_{i \rightarrow j, l}$ , we assume that sample  $(x_{i,l}, y_{i,l})$  is associated with MT  $m (\in \mathcal{M}_i)$ . Then we design

$$\phi_{i \rightarrow j, l} = \frac{r_{m,i \rightarrow j}}{t_d}, \quad j \in \mathcal{V}_i; \quad \phi_{i,l} = 1 - \frac{1}{t_d} \sum_{j \in \mathcal{V}_i} r_{m,i \rightarrow j}. \quad (28)$$

It is easy to verify that  $\phi_{i,l} + \sum_{j \in \mathcal{V}_i} \phi_{i \rightarrow j, l} = 1$ . We define an  $N \times N$  matrix  $\mathbf{c}$  with entries  $c_{i,j}$ , which satisfies  $\sum_j c_{i,j} \leq 1$ ,  $c_{i,j} = 0$  if  $j \notin \mathcal{V}_i$ ,  $\forall i \in \mathcal{V}$ . The matrix  $\mathbf{c}$  does not need to be symmetrical. We set the intertask combiners by

$$c_{i,j} = \begin{cases} \frac{1}{d_i} \left[ 1 - \exp\left(-v \sum_{m \in \mathcal{M}_i} r_{m,i \rightarrow j}\right) \right], & j \in \mathcal{V}_i; \\ 0, & j \notin \mathcal{V}_i, \end{cases} \quad (29)$$

where  $v$  is a positive constant.

In what follows, we will state the rationality of settings (28) and (29). From (26),  $\phi_{i,l}$  controls the importance of sample  $(x_{i,l}, y_{i,l})$  in parameter training at agent  $i$ . While  $\phi_{i \rightarrow j, l}$  controls the importance of  $(x_{i,l}, y_{i,l})$  on the transferred model parameter to agent  $j$ , which indirectly influence the output model parameters at agent  $j$ . Considering MT  $m \in \mathcal{M}_i$  related to  $(x_{i,l}, y_{i,l})$ , the sample will be more important for training the model at agent  $i$  if  $m$  is predicted to stay longer time during  $[0, t_d]$ . Hence a larger  $\phi_{i,l}$  is resulted. This also explains the choice of  $\phi_{i \rightarrow j, l}$ . On the other hand, the task combiner  $c_{i,j}$  decides the amount of information provided by agent  $i$  to  $j$ . If the flow of MTs from agent  $i$  to  $j$  is predicted to be dense, we set a large intertask combiner  $c_{i,j}$  to enforce the model parameter of  $j$  similar to the transferred  $\mathbf{w}_{i,j}^{\text{loc}}$ .

**Proposition 3.** *With intertask combiners and adaptive parameter designed at (28) and (29), (P2) and (P1) are consistent when there is no MT flow across areas.*

*Proof.* When there does not exist the transition of MTs among agents,  $r_{m,i \rightarrow j} = 0, \forall i \in \mathcal{V}, j \in \mathcal{V}_i$  and hence

$\phi_{i,l} = 1, \phi_{i \rightarrow j,l} = c_{i,j} = 0, \forall i \in \mathcal{V}, j \in \mathcal{V}_j, l = 1, \dots, b_i$ . Then  $\tilde{f}_i(\check{\mathbf{w}}_i, \hat{\mathbf{w}}_i) = f_i(\check{\mathbf{w}}_i, \hat{\mathbf{w}}_i)$  and (P2) reduces to (P1).  $\square$

---

**Algorithm 2:**


---

- 1: **initialize:** set  $\{\check{\mathbf{w}}_i^0, \hat{\mathbf{w}}_i^0 | i \in \mathcal{V}\}$  randomly and  $\lambda^0 = \mathbf{0}$ .
  - 2: **agents**  $i = 1$  to  $N$ :
  - 3: calculate  $\{\phi_{i,l}, \phi_{i \rightarrow j,l}, c_{i,j}, \mathbf{w}_{i,j}^{\text{loc}} | l = 1, \dots, b_i, j \in \mathcal{V}_i\}$  and communicate  $\mathbf{w}_{i,j}^{\text{loc}}$  to agent  $j \in \mathcal{V}_i$ .
  - 4: **for**  $k = 0, 1, \dots$  **do**
  - 5: follow steps 3-7 in Algorithm 1 but substituting  $\mathcal{L}_\rho^1$  with  $\mathcal{L}_\rho^2$ .
  - 6: **end for**
- 

The augmented Lagrange function for (P2) is given by

$$\mathcal{L}_\rho^2(\check{\mathbf{W}}, \hat{\mathbf{W}}, \lambda) = \sum_i \left( \tilde{f}_i(\check{\mathbf{w}}_i, \hat{\mathbf{w}}_i) + \frac{\mu_1}{2} \|\check{\mathbf{w}}_i\|^2 + \frac{\mu_2}{2} \|\hat{\mathbf{w}}_i\|^2 + \frac{\mu_3}{2} \sum_{j \in \mathcal{V}_i} c_{j,i} \|\mathbf{w}_{j,i}^{\text{loc}} - (\check{\mathbf{w}}_i + \hat{\mathbf{w}}_i)\|^2 + \lambda^T \mathbf{A} \check{\mathbf{W}} + \frac{\rho}{2} \|\mathbf{A} \check{\mathbf{W}}\|^2 \right). \quad (30)$$

Adopting hybrid Jacobi and Gauss-Seidel type ADMM as Algorithm 1, the update for (P2) follows (3)-(5) but substituting  $\mathcal{L}_\rho^1$  with  $\mathcal{L}_\rho^2$ . Then we provide Algorithm 2 to obtain the optimal solution for (P2). Compared with the process of Algorithm 1, the difference is that agent  $i (\in \mathcal{V})$  needs to calculate the transferred weights  $\mathbf{w}_{i,j}^{\text{loc}}$  first.

### C. Convergence Analysis

To analyze the convergence of Algorithm 2, we define

$$\mathbb{f}_i(\check{\mathbf{w}}_i, \hat{\mathbf{w}}_i) = \tilde{f}_i(\check{\mathbf{w}}_i, \hat{\mathbf{w}}_i) + \frac{\mu_3}{2} \sum_{j \in \mathcal{V}_i} c_{j,i} \|\mathbf{w}_{j,i}^{\text{loc}} - (\check{\mathbf{w}}_i + \hat{\mathbf{w}}_i)\|^2, \quad (31)$$

and  $\mathbb{F}(\check{\mathbf{W}}, \hat{\mathbf{W}}) = \sum_i (\mathbb{f}_i(\check{\mathbf{w}}_i, \hat{\mathbf{w}}_i) + g(\check{\mathbf{w}}_i) + h(\hat{\mathbf{w}}_i))$ . Then we follow the same argumentation as in the convergence proof for Algorithm 1.

**Assumption 3.**  $\tilde{f}_i$  and  $\tilde{f}_{i \rightarrow j}$  are differentiable and jointly convex over  $\check{\mathbf{w}}_i$  and  $\hat{\mathbf{w}}_i$ . The gradient  $\nabla \tilde{f}_i$  is Lipschitz continuous with constant  $\tilde{C}_i$ .

With Assumption 3, we can present the following property of  $\mathbb{f}_i$  by Lemma 3.

**Lemma 3.**  $\mathbb{f}_i$  satisfies Assumption 2 and Lemma 1 but with Lipschitz constant

$$\mathbb{C}_i = \sqrt{2\tilde{C}_i^2 + 4\mu_3^2 \left( \sum_{j \in \mathcal{V}_i} c_{j,i} \right)^2}. \quad (32)$$

*Proof.* See the Appendix E.  $\square$

**Theorem 2.** (Convergence of Algorithm 2) Following the conditions in Corollary 1, letting  $\tau_i$  satisfy (22) and

$$\zeta_i > \frac{\mathbb{C}_i}{m} (\mathbb{C}_i + m), \quad (33)$$

then the sequence  $\mathbf{u}^k$  generated by Algorithm 2 converges to the global optimal solution  $\mathbf{u}^*$  of problem (P2) with rate (21).

*Proof.* With Lemma 3, it can be proved similarly as Theorem 1 and Corollary 1 but substituting  $C_i$  with  $\mathbb{C}_i$ .  $\square$

It is worth noting that the conditions derived in Theorems 1 and 2, Corollary 1 and Propositions 1 and 2 are all sufficient to make Algorithms 1 and 2 converge. Moreover, the proofs can be extended to the matrix case  $\check{\mathbf{w}}_i, \hat{\mathbf{w}}_i \in \mathbb{R}^{n_1 \times n_2}$  by substituting the product  $a^T b$  by  $\langle a, b \rangle = \text{tr}(a^T b)$ .

## IV. SIMULATION AND DISCUSSION

In this section, we will provide simulations based on real dataset for the presented algorithms, and give discussions on the numerical results.

### A. Convergence Experiment

We first evaluate the convergence of Algorithms 1 and 2 by using the least square loss at agent  $i$  as

$$\ell(\check{\mathbf{w}}_i, \hat{\mathbf{w}}_i, x_{i,l}, y_{i,l}) = \frac{1}{2} \|(\check{\mathbf{w}}_i + \hat{\mathbf{w}}_i)^T x_{i,l} - y_{i,l}\|^2. \quad (34)$$

With (34) it is easy to verify that Assumptions 2 and 3 can be satisfied. Denoting  $X_i = [x_{i,1}, \dots, x_{i,b_i}]$  and  $Y_i = [y_{i,1}, \dots, y_{i,b_i}]$ , the local objective becomes  $f_i(\check{\mathbf{w}}_i, \hat{\mathbf{w}}_i) = \frac{1}{2b_i} \|(\check{\mathbf{w}}_i + \hat{\mathbf{w}}_i)^T X_i - Y_i\|^2$ .

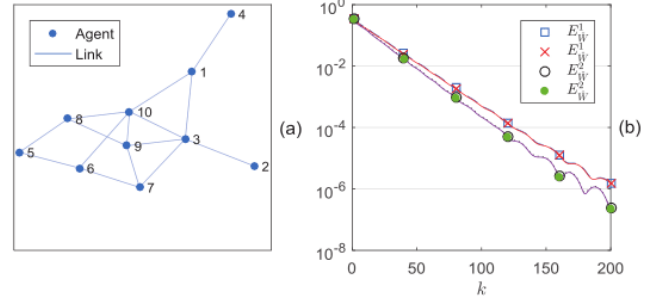


Fig. 2. (a) the connected graph  $\mathcal{G}$ ; (b) learning accuracy of Algorithms 1 and 2.

In the simulation setup, we let the number of agents  $N = 10$  with connections  $|\mathcal{E}| = 15$ , the number of training samples  $b_i = 10 (\forall i \in \mathcal{V})$ , input and output dimension  $n = 10, \nu = 1$ . The regularization parameters are  $\mu_1 = \mu_2 = \mu_3 = \mu_{12} = 1$  while step penalties are  $\tau_i = \zeta_i = 1$  and  $\rho = \gamma = 1$ . The connected graph  $\mathcal{G}$  is generated randomly shown as Fig. 2 (a). The entries of input  $x_{i,l}$  and output  $y_{i,l}$  are generated randomly according to uniform distribution  $\mathcal{U}(0, 1)$ . Besides, we generate  $\phi_{i \rightarrow j,l} \sim \mathcal{U}(0, \frac{1}{N})$  and hence  $\phi_{i,l} = 1 - \sum_{j \in \mathcal{V}_i} \phi_{i \rightarrow j,l}$ . The intertask combiners for agent  $i$  are generated by  $c_{i,j} \sim \mathcal{U}(0, \frac{1}{N}) (j \in \mathcal{V}_i)$ .

Denote the optimal solutions for (P1) and (P2) as  $\mathbf{u}_{\text{opt}}^1$  and  $\mathbf{u}_{\text{opt}}^2$  respectively, which are obtained by solving centralized cases for (P1) and (P2) with adopting Alternating Optimization (AO) method [46]. Then we define the accuracy with respect to  $\check{\mathbf{W}}$  and  $\hat{\mathbf{W}}$  in Algorithms 1 and 2 as

$$E_{\check{\mathbf{W}}}^{1,2}(k) = \sqrt{\frac{1}{Nn} \|\check{\mathbf{W}}^k - \check{\mathbf{W}}_{\text{opt}}^{1,2}\|^2}, \quad E_{\hat{\mathbf{W}}}^{1,2}(k) = \sqrt{\frac{1}{Nn} \|\hat{\mathbf{W}}^k - \hat{\mathbf{W}}_{\text{opt}}^{1,2}\|^2}, \quad (35)$$

which are shown in Fig. 2 (b). As we can observe, all the accuracy  $E_{\check{\mathbf{W}}}^{1,2}$  and  $E_{\hat{\mathbf{W}}}^{1,2}$  reduce with iteration  $k$ , which supports the convergence analysis in Theorems 1 and 2.

## B. Experiments on Real Dataset

The mobility prediction model based on the real trace data set *Geolife Trajectories* [47]–[49] is investigated. We select  $M = 20$  MTs out of the dataset with total 14587 paths. These paths were recorded during 9 months. As shown in Fig. 3 (a), the locations of MTs are exemplified based on GPS records (latitude and longitude), and some of the paths of each MT are shown in different colored dots respectively. The windowed area is roughly  $5 \times 5 \text{ km}^2$  large between latitude (39.97, 40.02) and longitude (116.30, 116.35). Assume that the agent  $i$  covers an square area with size  $\frac{5}{s} \times \frac{5}{s} \text{ km}^2$ . Then in considered region shown in Fig. 3 (a), we have agent  $N = s^2$ . Since traces of MT are repeated, the pmf  $\Psi_{m,i}(x)(i \in \mathcal{V})$  can be calculated statistically.

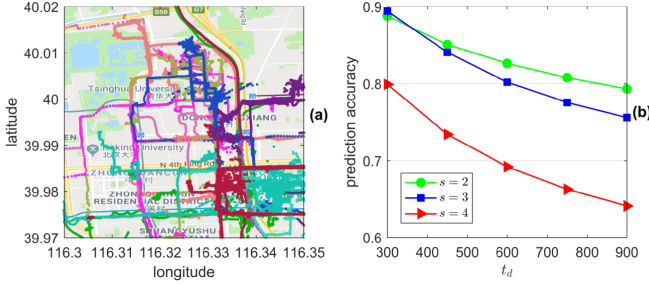


Fig. 3. (a) real traces of MTs; (b) accuracy of distributed mobility prediction based on *Markov renewal process* model.

In Fig. 3 (b), we verify the prediction accuracy of the *Markov renewal process* based mobility prediction model for these 20 MTs. We average the accuracy over MTs by conducting the prediction 100 times for the time window  $[0, t_d]$ . In prediction of MT  $m$ , we generate  $T_{m,0} \sim \Psi_{m,S_{m,0}}$ . We evaluate the prediction accuracy by counting the difference between real path and all the possible predicted paths, the detail of which can be found in [16]. As shown in Fig. 3 (b), the average accuracy for considered MTs degrades when we predict for a larger time window  $t_d$ , which is due to the increased uncertainty of MT mobility. Moreover, when the region is covered by more agents, e. g. with a smaller  $s$ , the prediction accuracy reduces. This is because increased agents may expand the number of possible paths within  $t_d$ . Thus it is harder to predict the movements. As a conclusion, for the considered  $t_d$  and  $s$ , the accuracy can be guaranteed at least 0.63 with the presented mobility model.

Then we evaluate the prediction results of Algorithms 1 and 2 with predicted moving patterns of MTs. We let  $F = 20$ ,  $s = 3$ ,  $K = 2$ ,  $t_i = 0.9$ ,  $t_d = 30 \text{ min}$  and randomly choose one path for each MT. Besides we generate  $T_{m,0} \sim \Psi_{m,S_{m,0}}$ . Each MT in  $\mathcal{M}$  is randomly assigned to one of the group in  $\mathcal{K}$ . The content preference for group  $i \in \mathcal{K}$  follows a Zipf-like distribution with shape parameter  $t_i$ ,

$$P_i(\pi_{i,f}) = \frac{f^{-t_i}}{\sum_{l \in \mathcal{F}} l^{-t_i}}, \quad i \in \mathcal{K}, \quad f \in \mathcal{F}, \quad (36)$$

where  $\pi_i$  is a random permutation of  $\mathcal{F}$  [26]. The content preference for two groups are presented in Fig. 4 (a). The

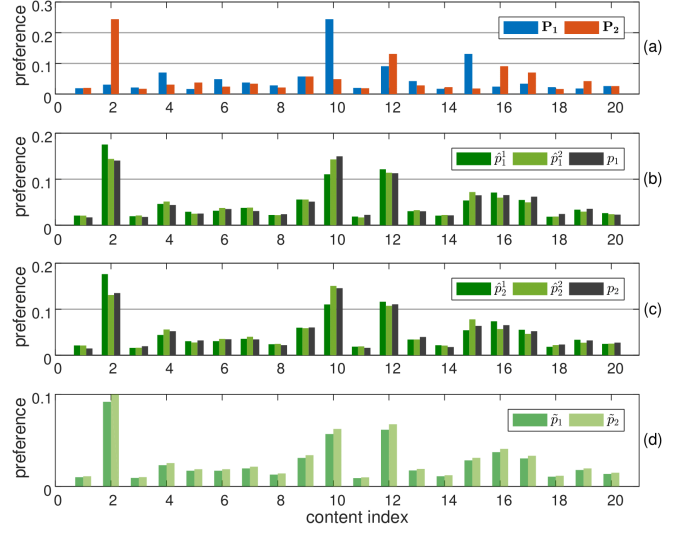


Fig. 4. (a) content preference for  $K = 2$  groups; (b), (c) predicted content preference  $\hat{p}_{1,2}^{1,2}$  by Algorithms 1 and 2, and observed preference  $p_{1,2}$  at agents 1 and 2; (d) common preference  $\tilde{p}_{1,2}$  predicted at agents 1 and 2.

dataset  $\mathcal{D}_i$  at agent  $i$  is collected in time  $[-t_d, 0]$ . We assume the request frequency for MTs is homogeneous as  $R_f = 2/\text{min}$ . Considering the sample  $(x_{i,l}, y_{i,l})$ , which is a record for one request at agent  $i$ , the  $x_{i,l}$  represents the feature of associated MT while  $y_{i,l}$  records the requested file. Without loss of generality, we assume the MTs with similar features have analogous preference. Hence we use the index of groups of MT to generate  $x_{i,l} \in \{0, 1\}^{K \times 1}$ , e.g., the associated MT belongs to group 1, then  $x_{i,l} = [1, 0]^T$  otherwise  $x_{i,l} = [0, 1]^T$ . We denote the target as  $y_{i,l} \in \{0, 1\}^{F \times 1}$ , e.g., if  $f$  is the requested file, then  $y_{i,l,f} = 1$  while the other elements are 0. We denote  $p_i$  as the content preference observed by agent  $i (\in \mathcal{V})$  during time  $[0, t_d]$ . We run Algorithms 1 and 2 for 300 iterations with parameter  $\mu_1 = \mu_2 = 0.1$ ,  $\mu_{12} = 0.01$ , while the other parameters are the same with previous subsection. The predicted content preference by agent  $i$  is calculated by  $\hat{p}_i^{1,2} = \frac{\sum_{m \in \mathcal{M}_i} (\tilde{w}_i^{1,2} + \hat{w}_i^{1,2})^T x_m}{\sum_{m \in \mathcal{M}_i} \mathbf{1} \cdot (\tilde{w}_i^{1,2} + \hat{w}_i^{1,2})^T x_m}$ , where  $\tilde{w}_i^{1,2}$  and  $\hat{w}_i^{1,2}$  are obtained by Algorithms 1 and 2 respectively and  $\mathbf{1} = [1, \dots, 1]$ .  $x_m (m \in \mathcal{M}_i)$  is the inputs observed at time 0 for agent  $i$ . In particular, we investigate the predicted preference for agents 1 and 2.  $p_{1,2}$  and  $\hat{p}_{1,2}^{1,2}$  are presented in Fig. 4 (b) and (c), which illustrate that without considering MTs mobility, both  $\hat{p}_1^1$  and  $\hat{p}_2^2$  make wrong prediction on the most popular content. But  $\hat{p}_1^2$  and  $\hat{p}_2^1$  can give accurate prediction. The common preference predicted at agent  $i$  with Algorithm 2 is given by  $\tilde{p}_i = \frac{\sum_{m \in \mathcal{M}_i} (\tilde{w}_i^2)^T x_m}{\sum_{m \in \mathcal{M}_i} \mathbf{1} \cdot (\tilde{w}_i^2)^T x_m}$ .  $\tilde{p}_1$  and  $\tilde{p}_2$  are shown in Fig. 4 (d). It demonstrates that the basis  $w_0$  learned jointly across agents can capture the common content interests.

Moreover, we average the prediction error on learned preference over the agents by carrying out the simulation for 100 times. The average estimation error of Algorithms 1 and 2 is defined by

$$\varepsilon^{1,2} = \frac{1}{N} \sum_{i \in \mathcal{V}} \|\hat{p}_i^{1,2} - p_i\|_1. \quad (37)$$

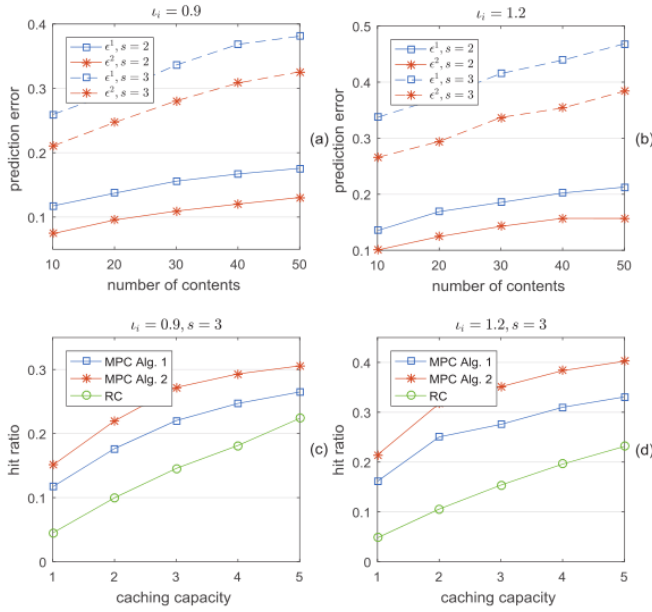


Fig. 5. (a), (b) geography preference prediction error with  $\iota_i = \{0.9, 1.2\}$ ; (c), (d) hit ratio of policies with  $\iota_i = \{0.9, 1.2\}$ ,  $s = 3$ .

As presented in Fig. 5 (a) and (b), the error of predicted geography preference achieved by the mobility-aware DRMTL model is always smaller than that of DRMTL. With growing  $F$ , the error  $\varepsilon^1$  and  $\varepsilon^2$  both exhibit an increasing trend. This is because more contents need to be predicted for a larger  $F$  but the number of training samples is fixed. Moreover, due to the fact that it is harder to learn a more concentrated preference without adequate data, the prediction performance of model (P1) and (P2) both become worse for a larger shape parameter, e.g.,  $\iota_i = 1.2$ . Hence from Fig. 4 and Fig. 5 (a), (b), we can conclude that  $\hat{p}_i^2$ , which is obtained by adaptively reweighting the learning samples from mobility patterns and transferring information across agents, can more accurately predict  $p_i$  than  $\hat{p}_i^1$  given by DRMTL model. This shows the feasibility of Algorithm 2 in real mobile applications.

Finally, we evaluate the average hit ratio defined in [17] for each agent, which represents the proportion of served requests by the caching of agents during time  $[0, t_d]$ . We assume the caching capacity for agents is  $\theta \in (\mathbb{N}_+)$  and  $\theta \leq F$ . In proactive caching, each agent stores the contents at time 0 according to the following two policies:

- 1) *Most popular caching* (MPC) [4]: each agent proactively stores content according to descending order of its predicted preference until  $\theta$  is occupied;
- 2) *Random caching* (RC) [4]: each agent proactively stores content in random manner until  $\theta$  is occupied.

For the MPC method, we consider two approaches, the Algorithms 1 and 2, to predict the content preference for agents. Since the stored contents are randomly selected for RC policy, there is no need to conduct the prediction of geography preference. In the simulation setup, we fix  $F = 20$  and  $s = 3$ . The results on hit ratio are demonstrated in Fig. 5 (c) and (d). It is seen that the hit ratio achieved by MPC with the geography preference predicted by mobility-aware DRMTL model can outperform the MPC with preference from Algorithm 1 and

RC scheme. Since more requests can be served by agent locally, with enlarging the caching capacity  $\theta$ , the hit ratio for all methods grow. The increase of RC follows a constant rate, while the rate of MPC policies degrade. This is expected since the contents proactively cached are randomly chosen in RC policy. But the MPC will choose to store those contents that are more likely to be requested, and the growth rate of cumulative preference for the cached contents will reduce with increasing  $\theta$ , which is caused by the nature of Zip-f like distribution. It is known that the preference of MTs become more concentrated when the shape parameter  $\iota_i$  gets larger. Hence with  $\iota_i = 1.2$ , the hit ratios achieved by all policies are better than that of  $\iota_i = 0.9$ . This does not violate the trends shown in Fig. 5 (a) and (b), where prediction error degrades with  $\iota_i$ , since only the index of descending order of predicted preference counts for the hit ratio in proactive caching problem.

## V. CONCLUSIONS

We study mobility-aware preference prediction for decentralized networks with heterogeneous interests for the MTs. The DRMTL model is first formulated to tackle the learning problem with stationary MTs, which is solved by the proposed proximal ADMM based Algorithm 1 in a hybrid Jacobian and Gauss-Seidel type. Then we extend the DRMTL model by reweighting training samples and introducing a transfer penalty in objective. With the modification, the mobility-aware DRMTL model, which is consistent with the DRMTL model, can successfully capture the variation of geography preference when mobility pattern of MTs is predictable. Our real trace driven simulation demonstrates that the MPC scheme with preference predicted by mobility-aware DRMTL model can achieve better performance on hit ratios than MPC with preference from DRMTL and RC scheme.

## APPENDIX A

### PROOF OF LEMMA 2

Define the intermediate variable as  $\mathbf{z}_i^{k+\frac{1}{2}} = [\check{\mathbf{w}}_i^{k+\frac{1}{2}}, \hat{\mathbf{w}}_i^k]$ . Then from three point inequality (7) in Lemma 1, we have

$$\begin{aligned} f_i(\mathbf{z}_i^{k+1}) - f_i(\mathbf{z}_i^*) &\leq (\mathbf{z}_i^{k+1} - \mathbf{z}_i^*)^T \nabla f_i(\mathbf{z}_i^{k+\frac{1}{2}}) + \frac{C_i}{2} \|\mathbf{z}_i^{k+1} - \mathbf{z}_i^{k+\frac{1}{2}}\|^2 \\ &= (\check{\mathbf{w}}_i^{k+1} - \check{\mathbf{w}}_i^*)^T \nabla_{\check{\mathbf{w}}_i} f_i(\mathbf{z}_i^{k+\frac{1}{2}}) + (\hat{\mathbf{w}}_i^{k+1} - \hat{\mathbf{w}}_i^*)^T \nabla_{\hat{\mathbf{w}}_i} f_i(\mathbf{z}_i^{k+\frac{1}{2}}) + \\ &\quad \frac{C_i}{2} \|\hat{\mathbf{w}}_i^k - \hat{\mathbf{w}}_i^{k+1}\|^2. \end{aligned} \quad (38)$$

Following (8) and (9) in Lemma 1, it is easy to show that

$$\begin{aligned} g(\check{\mathbf{w}}_i^{k+1}) - g(\check{\mathbf{w}}_i^*) &\leq (\check{\mathbf{w}}_i^{k+1} - \check{\mathbf{w}}_i^*)^T g'(\check{\mathbf{w}}_i^{k+1}), \\ h(\hat{\mathbf{w}}_i^{k+1}) - h(\hat{\mathbf{w}}_i^*) &\leq (\hat{\mathbf{w}}_i^{k+1} - \hat{\mathbf{w}}_i^*)^T h'(\hat{\mathbf{w}}_i^{k+1}) - \frac{m}{2} \|\hat{\mathbf{w}}_i^{k+1} - \hat{\mathbf{w}}_i^*\|^2. \end{aligned} \quad (39)$$

Meanwhile the KKT conditions are

$$\mathbf{A}\check{\mathbf{W}}^* = 0, \text{ and } \mathbf{A}_i^T \lambda^* = \nabla_{\check{\mathbf{w}}_i} F_i(\mathbf{z}_i^*), \quad \mathbf{0} = \nabla_{\hat{\mathbf{w}}_i} F_i(\mathbf{z}_i^*). \quad (40)$$

Furthermore, considering the convexity of  $F_i(\mathbf{z}_i)$  as (8), we have

$$F_i(\mathbf{z}_i^{k+1}) - F_i(\mathbf{z}_i^*) \geq (\mathbf{z}_i^{k+1} - \mathbf{z}_i^*)^T \nabla F_i(\mathbf{z}_i^*) = (\check{\mathbf{w}}_i^{k+1} - \check{\mathbf{w}}_i^*)^T \mathbf{A}_i^T \lambda^*. \quad (41)$$

Combining (38), (39), (40) and (41), we can obtain

$$\begin{aligned}
0 &\leq (\check{\mathbf{w}}_i^{k+1} - \check{\mathbf{w}}_i^*)^T (\nabla_{\check{\mathbf{w}}_i} F_i(\mathbf{z}_i^{k+\frac{1}{2}}) - A_i^T \lambda^*) + (\hat{\mathbf{w}}_i^{k+1} - \hat{\mathbf{w}}_i^*)^T \\
&\quad (\nabla_{\hat{\mathbf{w}}_i} F_i(\mathbf{z}_i^{k+1}) + \nabla_{\hat{\mathbf{w}}_i} f_i(\mathbf{z}_i^{k+\frac{1}{2}}) - \nabla_{\hat{\mathbf{w}}_i} f_i(\mathbf{z}_i^{k+1})) + \\
&\quad \frac{C_i}{2} \|\hat{\mathbf{w}}_i^k - \hat{\mathbf{w}}_i^{k+1}\|^2 - \frac{m}{2} \|\hat{\mathbf{w}}_i^{k+1} - \hat{\mathbf{w}}_i^*\|^2 \\
&\leq (\check{\mathbf{w}}_i^{k+1} - \check{\mathbf{w}}_i^*)^T (\nabla_{\check{\mathbf{w}}_i} F_i(\mathbf{z}_i^{k+\frac{1}{2}}) - A_i^T \lambda^*) + (\hat{\mathbf{w}}_i^{k+1} - \hat{\mathbf{w}}_i^*)^T \\
&\quad \nabla_{\hat{\mathbf{w}}_i} F_i(\mathbf{z}_i^{k+1}) + C_i \|\hat{\mathbf{w}}_i^{k+1} - \hat{\mathbf{w}}_i^*\| \|\hat{\mathbf{w}}_i^k - \hat{\mathbf{w}}_i^{k+1}\| + \\
&\quad \frac{C_i}{2} \|\hat{\mathbf{w}}_i^k - \hat{\mathbf{w}}_i^{k+1}\|^2 - \frac{m}{2} \|\hat{\mathbf{w}}_i^{k+1} - \hat{\mathbf{w}}_i^*\|^2 \\
&\stackrel{(a)}{\leq} (\check{\mathbf{w}}_i^{k+1} - \check{\mathbf{w}}_i^*)^T (\nabla_{\check{\mathbf{w}}_i} F_i(\mathbf{z}_i^{k+\frac{1}{2}}) - A_i^T \lambda^*) + (\hat{\mathbf{w}}_i^{k+1} - \hat{\mathbf{w}}_i^*)^T \\
&\quad \nabla_{\hat{\mathbf{w}}_i} F_i(\mathbf{z}_i^{k+1}) + \frac{C_i}{2m} (C_i + m) \|\hat{\mathbf{w}}_i^k - \hat{\mathbf{w}}_i^{k+1}\|^2,
\end{aligned} \tag{42}$$

where (a) is the inequality  $C_i \|\hat{\mathbf{w}}_i^{k+1} - \hat{\mathbf{w}}_i^*\| \|\hat{\mathbf{w}}_i^k - \hat{\mathbf{w}}_i^{k+1}\| \leq \frac{m}{2} \|\hat{\mathbf{w}}_i^{k+1} - \hat{\mathbf{w}}_i^*\|^2 + \frac{C_i^2}{2m} \|\hat{\mathbf{w}}_i^k - \hat{\mathbf{w}}_i^{k+1}\|^2$ . Recall the  $k$ -th iteration in Algorithm 1, agent  $i$  first solves (3), with the optimality conditions as

$$\begin{aligned}
&A_i^T [\lambda^k - \rho(A_i \check{\mathbf{w}}_i^{k+1} + \sum_{j \neq i} A_j \check{\mathbf{w}}_j^k)] + P_i (\check{\mathbf{w}}_i^k - \check{\mathbf{w}}_i^{k+1}) \\
&= A_i^T [\lambda^k + \rho A_i (\check{\mathbf{w}}_i^k - \check{\mathbf{w}}_i^{k+1}) - \rho \mathbf{A} (\check{\mathbf{W}}^k - \check{\mathbf{W}}^{k+1}) - \\
&\quad \rho \mathbf{A} (\check{\mathbf{W}}^{k+1} - \check{\mathbf{W}}^*)] + P_i (\check{\mathbf{w}}_i^k - \check{\mathbf{w}}_i^{k+1}) = \nabla_{\check{\mathbf{w}}_i} F_i(\mathbf{z}_i^{k+\frac{1}{2}}).
\end{aligned} \tag{43}$$

Then the agent  $i$  updates  $\hat{\mathbf{w}}_i$  by solving the subproblem (5). The optimality condition gives

$$Q_i (\hat{\mathbf{w}}_i^k - \hat{\mathbf{w}}_i^{k+1}) = \nabla_{\hat{\mathbf{w}}_i} F_i(\mathbf{z}_i^{k+1}). \tag{44}$$

Then by plugging (43) and (44) into (42), we have following inequality

$$\begin{aligned}
&(\check{\mathbf{w}}_i^{k+1} - \check{\mathbf{w}}_i^*)^T A_i^T (\lambda^k - \lambda^*) + (\check{\mathbf{w}}_i^{k+1} - \check{\mathbf{w}}_i^*)^T (\rho A_i^T A_i + P_i) \cdot \\
&(\check{\mathbf{w}}_i^k - \check{\mathbf{w}}_i^{k+1}) + (\hat{\mathbf{w}}_i^{k+1} - \hat{\mathbf{w}}_i^*)^T Q_i (\hat{\mathbf{w}}_i^k - \hat{\mathbf{w}}_i^{k+1}) \\
&\geq \rho (\check{\mathbf{w}}_i^{k+1} - \check{\mathbf{w}}_i^*)^T A_i^T \mathbf{A} (\check{\mathbf{W}}^k - \check{\mathbf{W}}^{k+1}) - \frac{C_i}{2m} (C_i + m) \cdot \\
&\quad \|\hat{\mathbf{w}}_i^k - \hat{\mathbf{w}}_i^{k+1}\|^2 + \rho (\check{\mathbf{w}}_i^{k+1} - \check{\mathbf{w}}_i^*)^T A_i^T \mathbf{A} (\check{\mathbf{W}}^{k+1} - \check{\mathbf{W}}^*).
\end{aligned} \tag{45}$$

Since  $\lambda^{k+1} = \lambda^k - \gamma \rho \mathbf{A} \check{\mathbf{W}}^{k+1}$ , it can be derived that

$$\mathbf{A} (\check{\mathbf{W}}^{k+1} - \check{\mathbf{W}}^*) = \frac{1}{\gamma \rho} (\lambda^k - \lambda^{k+1}). \tag{46}$$

Noting the truth that  $\lambda^k - \lambda^* = \lambda^k - \lambda^{k+1} + \lambda^{k+1} - \lambda^*$ , and summing the inequality (45) over all  $i \in \mathcal{V}$ , we obtain

$$\begin{aligned}
&\frac{1}{\gamma \rho} (\lambda^k - \lambda^{k+1})^T (\lambda^k - \lambda^*) + \sum_i [(\check{\mathbf{w}}_i^{k+1} - \check{\mathbf{w}}_i^*)^T (\rho A_i^T A_i + P_i) \cdot \\
&(\check{\mathbf{w}}_i^k - \check{\mathbf{w}}_i^{k+1}) + (\hat{\mathbf{w}}_i^{k+1} - \hat{\mathbf{w}}_i^*)^T Q_i (\hat{\mathbf{w}}_i^k - \hat{\mathbf{w}}_i^{k+1})] \\
&\geq \frac{1-\gamma}{\gamma^2 \rho} \|\lambda^k - \lambda^{k+1}\|^2 + \frac{1}{\gamma} (\lambda^k - \lambda^{k+1})^T \mathbf{A} (\check{\mathbf{W}}^k - \check{\mathbf{W}}^{k+1}) - \\
&\quad \sum_i \frac{C_i}{2m} (C_i + m) \|\hat{\mathbf{w}}_i^k - \hat{\mathbf{w}}_i^{k+1}\|^2,
\end{aligned} \tag{47}$$

or more compactly,

$$\begin{aligned}
(\mathbf{u}^k - \mathbf{u}^{k+1})^T \mathbf{G} (\mathbf{u}^{k+1} - \mathbf{u}^*) &\geq \frac{1-\gamma}{\gamma^2 \rho} \|\lambda^k - \lambda^{k+1}\|^2 + \\
\frac{1}{\gamma} (\lambda^k - \lambda^{k+1})^T \mathbf{A} (\check{\mathbf{W}}^k - \check{\mathbf{W}}^{k+1}) &- \sum_i \frac{C_i}{2m} (C_i + m) \|\hat{\mathbf{w}}_i^k - \hat{\mathbf{w}}_i^{k+1}\|^2.
\end{aligned} \tag{48}$$

With the equality  $\|\mathbf{u}^k - \mathbf{u}^*\|_{\mathbf{G}}^2 - \|\mathbf{u}^{k+1} - \mathbf{u}^*\|_{\mathbf{G}}^2 = 2(\mathbf{u}^k - \mathbf{u}^{k+1})^T \mathbf{G} (\mathbf{u}^{k+1} - \mathbf{u}^*) + \|\mathbf{u}^k - \mathbf{u}^{k+1}\|_{\mathbf{G}}^2$ , we can get the desired result as

$$\begin{aligned}
\|\mathbf{u}^k - \mathbf{u}^*\|_{\mathbf{G}}^2 - \|\mathbf{u}^{k+1} - \mathbf{u}^*\|_{\mathbf{G}}^2 &\geq \frac{2-\gamma}{\gamma^2 \rho} \|\lambda^k - \lambda^{k+1}\|^2 + \\
\frac{2}{\gamma} (\lambda^k - \lambda^{k+1})^T \mathbf{A} (\check{\mathbf{W}}^k - \check{\mathbf{W}}^{k+1}) &+ \|\check{\mathbf{W}}^k - \check{\mathbf{W}}^{k+1}\|_{\mathbf{G}_1}^2 + \\
\|\check{\mathbf{W}}^k - \check{\mathbf{W}}^{k+1}\|_{\mathbf{G}_2 - \mathbf{G}_3}^2 &= \|\mathbf{u}^k - \mathbf{u}^{k+1}\|_{\mathbf{M}}^2.
\end{aligned} \tag{49}$$

## APPENDIX B

### PROOF OF THEOREM 1

To prove the convergence of Alg.1, we should ensure that  $\|\mathbf{u}\|_{\mathbf{M}}^2 \geq 0$  holds for any  $\mathbf{u}$ , which is equivalent to guaranteeing  $\mathbf{M}$  to be semi-positive. We have

$$\|\mathbf{u}\|_{\mathbf{M}}^2 = \|\check{\mathbf{W}}\|_{\mathbf{G}_1}^2 + \|\hat{\mathbf{W}}\|_{\mathbf{G}_2 - \mathbf{G}_3}^2 + \frac{2-\gamma}{\gamma^2 \rho} \|\lambda\|^2 + \frac{2}{\gamma} \lambda^T \mathbf{A} \check{\mathbf{W}}. \tag{50}$$

Moreover, we can derive the following inequality

$$\frac{2}{\gamma} \lambda^T \mathbf{A} \check{\mathbf{W}} = \sum_i \lambda^T A_i \check{\mathbf{w}}_i \geq - \sum_i \left( \frac{\epsilon_i}{\gamma^2 \rho} \|\lambda\|^2 + \frac{\rho}{\epsilon_i} \|A_i \check{\mathbf{w}}_i\|^2 \right)^2, \tag{51}$$

where  $\epsilon_i > 0$ . Hence putting (51) into (50), we can obtain

$$\begin{aligned}
\|\mathbf{u}\|_{\mathbf{M}}^2 &\geq \sum_i \left( \|\check{\mathbf{w}}_i\|_{P_i + \rho(1 - \frac{1}{\epsilon_i}) A_i^T A_i}^2 + \|\hat{\mathbf{w}}_i\|_{Q_i - \frac{C_i}{m} (C_i + m) I}^2 \right) + \\
&\quad \frac{2-\gamma - \sum_i \epsilon_i}{\gamma^2 \rho} \|\lambda\|^2.
\end{aligned} \tag{52}$$

Since  $A_i^T A_i = d_i I$ , guaranteeing that  $P_i + \rho(1 - \frac{1}{\epsilon_i}) d_i I > 0$ ,  $Q_i - \frac{C_i}{m} (C_i + m) I > 0$  and  $2-\gamma - \sum_i \epsilon_i > 0$ , makes  $\mathbf{M}$  positive definite and  $\|\mathbf{u}\|_{\mathbf{M}}^2 \geq 0$ . Hence the sequence  $\mathbf{u}^k$  converges to  $\mathbf{u}^*$  as  $k \rightarrow \infty$  according to [33]. Since  $P_i = \tau_i I$  and  $Q_i = \zeta_i I$ , we get the final results as (18).

## APPENDIX C

### PROOF OF COROLLARY 1

Combining (38), (39), (40), (43), (44) and summing over all  $i$ , we can get

$$\begin{aligned}
\mathbf{F}(\mathbf{Z}^{k+1}) - \mathbf{F}(\mathbf{Z}^*) &\leq \sum_i \left[ (\check{\mathbf{w}}_i^{k+1} - \check{\mathbf{w}}_i^*)^T \nabla_{\check{\mathbf{w}}_i} F_i(\mathbf{z}_i^{k+\frac{1}{2}}) + \right. \\
&(\hat{\mathbf{w}}_i^{k+1} - \hat{\mathbf{w}}_i^*)^T \nabla_{\hat{\mathbf{w}}_i} F_i(\mathbf{z}_i^{k+1}) + \frac{C_i}{2m} (C_i + m) \|\hat{\mathbf{w}}_i^k - \hat{\mathbf{w}}_i^{k+1}\|^2 \left. \right] \\
&= (\check{\mathbf{W}}^{k+1} - \check{\mathbf{W}}^*)^T (\mathbf{G}_1 - \rho \mathbf{A}^T \mathbf{A}) (\check{\mathbf{W}}^k - \check{\mathbf{W}}^{k+1}) + \\
&(\hat{\mathbf{W}}^{k+1} - \hat{\mathbf{W}}^*)^T \mathbf{G}_2 (\hat{\mathbf{W}}^k - \hat{\mathbf{W}}^{k+1}) + \frac{1}{2} \|\hat{\mathbf{W}}^k - \hat{\mathbf{W}}^{k+1}\|_{\mathbf{G}_3}^2 + \\
&\frac{1}{\gamma \rho} (\lambda^k - \lambda^{k+1})^T \lambda^k - \frac{1}{\gamma^2 \rho} \|\lambda^k - \lambda^{k+1}\|^2.
\end{aligned} \tag{53}$$

With the condition  $\mathbf{G}_1^\dagger = \mathbf{G}_1 - \rho \mathbf{A}^T \mathbf{A} > 0$ , we have

$$\|\check{\mathbf{W}}^k - \check{\mathbf{W}}^{k+1}\|_{\mathbf{G}_1^\dagger}^2 \geq 0. \quad (54)$$

While with  $\mathbf{G}_2 > \mathbf{G}_3$ , we can get

$$\|\hat{\mathbf{W}}^k - \hat{\mathbf{W}}^{k+1}\|_{\mathbf{G}_2}^2 \geq \|\hat{\mathbf{W}}^k - \hat{\mathbf{W}}^{k+1}\|_{\mathbf{G}_3}^2. \quad (55)$$

Moreover, for the last two terms in (53), we can derive

$$\begin{aligned} & \frac{1}{\gamma\rho} (\lambda^k - \lambda^{k+1})^T \lambda^k - \frac{1}{\gamma^2\rho} \|\lambda^k - \lambda^{k+1}\|^2 \\ &= \frac{1}{2\gamma\rho} \|\lambda^k - \lambda^{k+1}\|^2 + \frac{1}{2\gamma\rho} (\lambda^k - \lambda^{k+1})^T (\lambda^k + \lambda^{k+1}) - \\ & \frac{1}{\gamma^2\rho} \|\lambda^k - \lambda^{k+1}\|^2 \stackrel{(a)}{\leq} \frac{1}{2\gamma\rho} (\|\lambda^k\|^2 - \|\lambda^{k+1}\|^2), \end{aligned} \quad (56)$$

where (a) is because  $0 < \gamma < 2$ . The following result can be obtained by integrating (53), (54), (55) and (56) as

$$\begin{aligned} \mathbf{F}(\mathbf{Z}^{k+1}) - \mathbf{F}(\mathbf{Z}^*) &\leq (\mathbf{Z}^k - \mathbf{Z}^{k+1})^T \mathbf{G}_{12}^\dagger (\mathbf{Z}^{k+1} - \mathbf{Z}^*) + \\ & \frac{1}{2} \|\mathbf{Z}^k - \mathbf{Z}^{k+1}\|_{\mathbf{G}_{12}^\dagger}^2 + \frac{1}{2\gamma\rho} (\|\lambda^k\|^2 - \|\lambda^{k+1}\|^2) \\ &= \frac{1}{2} \left[ \|\mathbf{Z}^k - \mathbf{Z}^*\|_{\mathbf{G}_{12}^\dagger}^2 - \|\mathbf{Z}^{k+1} - \mathbf{Z}^*\|_{\mathbf{G}_{12}^\dagger}^2 + \frac{1}{\gamma\rho} (\|\lambda^k\|^2 - \|\lambda^{k+1}\|^2) \right], \end{aligned} \quad (57)$$

where  $\mathbf{G}_{12}^\dagger := \text{blkdiag}(\mathbf{G}_1^\dagger, \mathbf{G}_2)$ . Summing the above inequality over  $i = 1, \dots, k$ , we get

$$\begin{aligned} \mathbf{F}(\bar{\mathbf{Z}}^k) - \mathbf{F}(\mathbf{Z}^*) &\stackrel{(a)}{\leq} \frac{1}{k} \sum_{j=1}^k \mathbf{F}(\mathbf{Z}^j) - \mathbf{F}(\mathbf{Z}^*) \\ &\leq \frac{1}{2k} \left( \|\check{\mathbf{W}}^0 - \check{\mathbf{W}}^*\|_{\mathbf{G}_1^\dagger}^2 + \|\hat{\mathbf{W}}^0 - \hat{\mathbf{W}}^*\|_{\mathbf{G}_2}^2 + \frac{1}{\gamma\rho} \|\lambda^0\|^2 \right), \end{aligned} \quad (58)$$

where (a) is from the convexity of objective  $\mathbf{F}$ . Letting  $\lambda^0 = \mathbf{0}$  completes the proof.

#### APPENDIX D PROOF OF PROPOSITION 2

Considering the setting up for  $A_i$ , it can be deduced that  $A_i^T A_j = -I_{n \times n}$  if  $(i, j) \in \mathcal{E}$  otherwise  $A_i^T A_j = \mathbf{0}$ . Hence we can conclude  $\|A_i^T A_j\| \leq \sqrt{n}$ . Since  $\mathbf{G}_1^\dagger > 0$  and  $\mathbf{G}_2 > \mathbf{G}_3$  are required from the proof of Corollary 1, for any  $\check{\mathbf{W}}$  we need guarantee that

$$\begin{aligned} \|\check{\mathbf{W}}\|_{\mathbf{G}_1^\dagger}^2 &= \sum_i (\check{\mathbf{w}}_i^T P_i \check{\mathbf{w}}_i - \rho \sum_j \check{\mathbf{w}}_i^T A_i^T A_j \check{\mathbf{w}}_j) \\ &= \sum_i [\check{\mathbf{w}}_i^T (P_i - \rho A_i^T A_i) \check{\mathbf{w}}_i - \rho \sum_{j \neq i} \check{\mathbf{w}}_i^T A_i^T A_j \check{\mathbf{w}}_j] \\ &\stackrel{(a)}{\geq} \sum_i [\check{\mathbf{w}}_i^T (P_i - \rho A_i^T A_i) \check{\mathbf{w}}_i - \rho \sqrt{n} \sum_{j \neq i} \|\check{\mathbf{w}}_i\| \|\check{\mathbf{w}}_j\|] \\ &\geq \sum_i \|\check{\mathbf{w}}_i\|_{P_i - \rho A_i^T A_i - 4(N-1)\rho\sqrt{n}I}^2 \geq 0, \end{aligned} \quad (59)$$

where (a) is because  $\|A_i^T A_j\| \leq \sqrt{n}$  ( $i \neq j$ ). The inequality (59) can be satisfied if  $P_i - \rho A_i^T A_i - 4(N-1)\rho\sqrt{n}I > 0$ . With  $P_i = \tau_i I$  and  $A_i^T A_i = d_i I$ , it reduces to  $\tau_i > \rho d_i + 4(N-1)\rho\sqrt{n}$ . The condition for  $Q_i$  required in Corollary 1 are consistent with that in Theorem 1. Combining the results in Remark 1 completes the proof.

#### APPENDIX E PROOF OF LEMMA 3

From Assumption 3 we know  $\tilde{f}_i^j$  is jointly convex over  $\check{\mathbf{w}}_i$  and  $\hat{\mathbf{w}}_i$ . Thus with the convexity of term  $\|\mathbf{w}_{j,i}^{\text{loc}} - (\check{\mathbf{w}}_i + \hat{\mathbf{w}}_i)\|^2$  in (31), we can conclude that  $\mathbb{f}_i$  is differentiable and convex. The gradient of  $\nabla \tilde{f}_i$  satisfies

$$\|\nabla \tilde{f}_i(\mathbf{z}_i^1) - \nabla \tilde{f}_i(\mathbf{z}_i^2)\| \leq \tilde{C}_i \|\mathbf{z}_i^1 - \mathbf{z}_i^2\|, \quad \mathbf{z}_i^1, \mathbf{z}_i^2 \in \mathbb{R}^n \times \mathbb{R}^n. \quad (60)$$

Considering the partial gradient of  $\mathbb{f}_i$  over  $\check{\mathbf{w}}_i$ , we can derive the following inequality.

$$\begin{aligned} \|\partial \mathbb{f}_i(\mathbf{z}_i^1) - \partial \mathbb{f}_i(\mathbf{z}_i^2)\|^2 &= \|\partial \tilde{f}_i(\mathbf{z}_i^1) - \partial \tilde{f}_i(\mathbf{z}_i^2) + \mu_3 \sum_{j \in \mathcal{V}_i} c_{j,i} \cdot \\ & (\check{\mathbf{w}}_i^1 - \check{\mathbf{w}}_i^2 + \hat{\mathbf{w}}_i^1 - \hat{\mathbf{w}}_i^2)\|^2 \leq 2\|\partial \tilde{f}_i(\mathbf{z}_i^1) - \partial \tilde{f}_i(\mathbf{z}_i^2)\|^2 + 2\mu_3^2 \cdot \\ & \left( \sum_{j \in \mathcal{V}_i} c_{j,i} \right)^2 \|\check{\mathbf{w}}_i^1 - \check{\mathbf{w}}_i^2 + \hat{\mathbf{w}}_i^1 - \hat{\mathbf{w}}_i^2\|^2. \end{aligned} \quad (61)$$

Since  $\|\check{\mathbf{w}}_i^1 - \check{\mathbf{w}}_i^2 + \hat{\mathbf{w}}_i^1 - \hat{\mathbf{w}}_i^2\|^2 \leq 2(\|\check{\mathbf{w}}_i^1 - \check{\mathbf{w}}_i^2\|^2 + \|\hat{\mathbf{w}}_i^1 - \hat{\mathbf{w}}_i^2\|^2) = 2\|\mathbf{z}_i^1 - \mathbf{z}_i^2\|^2$ , summing the inequality (61) over partial gradient over  $\check{\mathbf{w}}_i$  and  $\hat{\mathbf{w}}_i$ , we obtain

$$\begin{aligned} \|\nabla \mathbb{f}_i(\mathbf{z}_i^1) - \nabla \mathbb{f}_i(\mathbf{z}_i^2)\|^2 &\leq 2\|\nabla \tilde{f}_i(\mathbf{z}_i^1) - \nabla \tilde{f}_i(\mathbf{z}_i^2)\|^2 + 4\mu_3^2 \cdot \\ & \left( \sum_{j \in \mathcal{V}_i} c_{j,i} \right)^2 \|\mathbf{z}_i^1 - \mathbf{z}_i^2\|^2 \\ &\leq \left[ 2\tilde{C}_i^2 + 4\mu_3^2 \left( \sum_{j \in \mathcal{V}_i} c_{j,i} \right)^2 \right] \|\mathbf{z}_i^1 - \mathbf{z}_i^2\|^2. \end{aligned} \quad (62)$$

We let  $\mathbb{C}_i = \sqrt{2\tilde{C}_i^2 + 4\mu_3^2 \left( \sum_{j \in \mathcal{V}_i} c_{j,i} \right)^2}$  to make (6) satisfied for  $\mathbb{f}_i$ . Then following the proof of Lemma 1, it can be shown that (7) also holds for  $\mathbb{f}_i$  but replacing  $C_i$  with  $\mathbb{C}_i$ .

#### REFERENCES

- [1] X. Wang, M. Chen, T. Taleb, A. Ksentini, and V. C. M. Leung, "Cache in the air: exploiting content caching and delivery techniques for 5g systems," *IEEE Communications Magazine*, vol. 52, no. 2, pp. 131–139, February 2014.
- [2] E. Bastug, M. Bennis, and M. Debbah, "Living on the edge: The role of proactive caching in 5g wireless networks," *IEEE Communications Magazine*, vol. 52, no. 8, pp. 82–89, Aug 2014.
- [3] D. Malak, M. Al-Shalash, and J. G. Andrews, "Optimizing content caching to maximize the density of successful receptions in device-to-device networking," *IEEE Transactions on Communications*, vol. 64, no. 10, pp. 4365–4380, Oct 2016.
- [4] R. Wang, X. Peng, J. Zhang, and K. B. Letaief, "Mobility-aware caching for content-centric wireless networks: modeling and methodology," *IEEE Communications Magazine*, vol. 54, no. 8, pp. 77–83, August 2016.
- [5] N. Golrezaei, P. Mansourifard, A. F. Molisch, and A. G. Dimakis, "Base-station assisted device-to-device communications for high-throughput wireless video networks," *IEEE Transactions on Wireless Communications*, vol. 13, no. 7, pp. 3665–3676, July 2014.
- [6] S. Krishnan and H. S. Dhillon, "Effect of user mobility on the performance of device-to-device networks with distributed caching," *IEEE Wireless Communications Letters*, vol. 6, no. 2, pp. 194–197, April 2017.
- [7] R. Wang, J. Zhang, S. H. Song, and K. B. Letaief, "Exploiting mobility in cache-assisted d2d networks: Performance analysis and optimization," *IEEE Transactions on Wireless Communications*, vol. 17, no. 8, pp. 5592–5605, Aug 2018.
- [8] K. Poularakis and L. Tassioulas, "Exploiting user mobility for wireless content delivery," in *2013 IEEE International Symposium on Information Theory*, July 2013, pp. 1017–1021.
- [9] E. Ozfatura and D. Gunduz, "Mobility and popularity-aware coded small-cell caching," *IEEE Communications Letters*, vol. 22, no. 2, pp. 288–291, Feb 2018.

- [10] M. Chen, W. Saad, C. Yin, and M. Debbah, "Echo state networks for proactive caching in cloud-based radio access networks with mobile users," *IEEE Transactions on Wireless Communications*, vol. 16, no. 6, pp. 3520–3535, June 2017.
- [11] R. Wang, J. Zhang, S. H. Song, and K. B. Letaief, "Exploiting mobility in cache-assisted d2d networks: Performance analysis and optimization," *IEEE Transactions on Wireless Communications*, vol. 17, no. 8, pp. 5592–5605, Aug 2018.
- [12] W. Zhang, D. Wu, W. Yang, and Y. Cai, "Caching on the move: A user interest-driven caching strategy for d2d content sharing," *IEEE Transactions on Vehicular Technology*, vol. 68, no. 3, pp. 2958–2971, March 2019.
- [13] L. T. Tan and R. Q. Hu, "Mobility-aware edge caching and computing in vehicle networks: A deep reinforcement learning," *IEEE Transactions on Vehicular Technology*, vol. 67, no. 11, pp. 10190–10203, Nov 2018.
- [14] S. Hosny, A. Eryilmaz, A. A. Abouzeid, and H. El Gamal, "Mobility-aware centralized d2d caching networks," in *2016 54th Annual Allerton Conference on Communication, Control, and Computing (Allerton)*, Sep. 2016, pp. 725–732.
- [15] X. Liu, J. Zhang, X. Zhang, and W. Wang, "Mobility-aware coded probabilistic caching scheme for mec-enabled small cell networks," *IEEE Access*, vol. 5, pp. 17824–17833, 2017.
- [16] Y. Ye, M. Xiao, Z. Zhang, and Z. Ma, "Performance analysis of mobility prediction based proactive wireless caching," in *2018 IEEE Wireless Communications and Networking Conference (WCNC)*, April 2018, pp. 1–6.
- [17] M. Chen, Y. Hao, L. Hu, K. Huang, and V. K. N. Lau, "Green and mobility-aware caching in 5g networks," *IEEE Transactions on Wireless Communications*, vol. 16, no. 12, pp. 8347–8361, Dec 2017.
- [18] L. Breslau, G. Phillips, and S. Shenker, "Web caching and zipf-like distributions: evidence and implications," in *1999 Proceedings IEEE INFOCOM*, vol. 1, March 1999, pp. 126–134 vol.1.
- [19] B. N. Bharath, K. G. Nagananda, and H. V. Poor, "A learning-based approach to caching in heterogeneous small cell networks," *IEEE Transactions on Communications*, vol. 64, no. 4, pp. 1674–1686, April 2016.
- [20] S. M. S. Tanzil, W. Hoiles, and V. Krishnamurthy, "Adaptive scheme for caching youtube content in a cellular network: Machine learning approach," *IEEE Access*, vol. 5, pp. 5870–5881, 2017.
- [21] S. Muller, O. Atan, M. van der Schaar, and A. Klein, "Context-aware proactive content caching with service differentiation in wireless networks," *IEEE Transactions on Wireless Communications*, vol. 16, no. 2, pp. 1024–1036, Feb 2017.
- [22] B. Chen and C. Yang, "Caching policy for cache-enabled d2d communications by learning user preference," *IEEE Transactions on Communications*, vol. 66, no. 12, pp. 6586–6601, Dec 2018.
- [23] Y. Jiang, M. Ma, M. Bennis, F. Zheng, and X. You, "User preference learning-based edge caching for fog radio access network," *IEEE Transactions on Communications*, vol. 67, no. 2, pp. 1268–1283, Feb 2019.
- [24] J. Song, M. Sheng, T. Q. S. Quek, C. Xu, and X. Wang, "Learning-based content caching and sharing for wireless networks," *IEEE Transactions on Communications*, vol. 65, no. 10, pp. 4309–4324, Oct 2017.
- [25] B. Blaszczyszyn and A. Giovanidis, "Optimal geographic caching in cellular networks," in *2015 IEEE International Conference on Communications (ICC)*, June 2015, pp. 3358–3363.
- [26] Y. Guo, L. Duan, and R. Zhang, "Cooperative local caching under heterogeneous file preferences," *IEEE Transactions on Communications*, vol. 65, no. 1, pp. 444–457, Jan 2017.
- [27] S. Borst, V. Gupta, and A. Walid, "Distributed caching algorithms for content distribution networks," in *2010 Proceedings IEEE INFOCOM*, March 2010, pp. 1–9.
- [28] L. Marini, J. Li, and Y. Li, "Distributed caching based on decentralized learning automata," in *2015 IEEE International Conference on Communications (ICC)*, June 2015, pp. 3807–3812.
- [29] J. Liu, B. Bai, J. Zhang, and K. B. Letaief, "Content caching at the wireless network edge: A distributed algorithm via belief propagation," in *2016 IEEE International Conference on Communications (ICC)*, May 2016, pp. 1–6.
- [30] Y. Ye, Z. Zhang, G. Yang, and M. Xiao, "Minimum cost based clustering scheme for cooperative wireless caching network with heterogeneous file preference," in *2017 IEEE International Conference on Communications (ICC)*, May 2017, pp. 1–6.
- [31] Z. Chen, J. Lee, T. Q. S. Quek, and M. Kountouris, "Cooperative caching and transmission design in cluster-centric small cell networks," *IEEE Transactions on Wireless Communications*, vol. 16, no. 5, pp. 3401–3415, May 2017.
- [32] T. Evgeniou and M. Pontil, "Regularized multi-task learning," in *Proceedings of the Tenth ACM SIGKDD International Conference on Knowledge Discovery and Data Mining*, ser. KDD '04. New York, NY, USA: ACM, 2004, pp. 109–117.
- [33] W. Deng, M.-J. Lai, Z. Peng, and W. Yin, "Parallel multi-block admm with  $\mathcal{O}(1/k)$  convergence," *Journal of Scientific Computing*, vol. 71, no. 2, pp. 712–736, May 2017.
- [34] Y. Cui, X. Li, D. Sun, and K.-C. Toh, "On the convergence properties of a majorized alternating direction method of multipliers for linearly constrained convex optimization problems with coupled objective functions," *J. Optim. Theory Appl.*, vol. 169, no. 3, pp. 1013–1041, Jun. 2016.
- [35] X. Gao and S.-Z. Zhang, "First-order algorithms for convex optimization with nonseparable objective and coupled constraints," *Journal of the Operations Research Society of China*, vol. 5, no. 2, pp. 131–159, Jun 2017.
- [36] Y. Xu, "Hybrid jacobian and gauss–seidel proximal block coordinate update methods for linearly constrained convex programming," *SIAM Journal on Optimization*, vol. 28, no. 1, pp. 646–670, 2018.
- [37] Y. Ye, M. Xiao, and M. Skoglund, "Decentralized multi-task learning based on extreme learning machines," *arXiv preprint arXiv:1904.11366*, 2019.
- [38] Y. Drori, S. Sabach, and M. Teboulle, "A simple algorithm for a class of nonsmooth convex-concave saddle-point problems," *Oper. Res. Lett.*, vol. 43, no. 2, pp. 209–214, Mar. 2015.
- [39] B. He, "A class of projection and contraction methods for monotone variational inequalities," *Applied Mathematics and Optimization*, vol. 35, no. 1, pp. 69–76, Jan 1997.
- [40] J.-K. Lee and J. C. Hou, "Modeling steady-state and transient behaviors of user mobility: Formulation, analysis, and application," in *Proceedings of the 7th ACM International Symposium on Mobile Ad Hoc Networking and Computing*. New York, NY, USA: ACM, 2006, pp. 85–96.
- [41] S. Akoush and A. Sameh, "Mobile user movement prediction using bayesian learning for neural networks," in *Proceedings of the 2007 International Conference on Wireless Communications and Mobile Computing*, ser. IWCMC '07. New York, NY, USA: ACM, 2007, pp. 191–196.
- [42] S. Scellato, M. Musolesi, C. Mascolo, V. Latora, and A. T. Campbell, "Nextplace: a spatio-temporal prediction framework for pervasive systems," in *International Conference on Pervasive Computing*. Springer, 2011, pp. 152–169.
- [43] S. Gambs, M.-O. Killijian, and M. N. del Prado Cortez, "Next place prediction using mobility markov chains," in *Proceedings of the First Workshop on Measurement, Privacy, and Mobility*. ACM, 2012, p. 3.
- [44] M. Ren, W. Zeng, B. Yang, and R. Urtasun, "Learning to reweight examples for robust deep learning," in *Proceedings of the 35th International Conference on Machine Learning*, J. Dy and A. Krause, Eds., vol. 80. PMLR, 10–15 Jul 2018, pp. 4334–4343.
- [45] C. Li, S. Huang, Y. Liu, and Y. Liu, "Distributed tls over multitask networks with adaptive intertask cooperation," *IEEE Transactions on Aerospace and Electronic Systems*, vol. 52, no. 6, pp. 3036–3052, December 2016.
- [46] A. Beck, "On the convergence of alternating minimization for convex programming with applications to iteratively reweighted least squares and decomposition schemes," *SIAM Journal on Optimization*, vol. 25, pp. 185–209, 2015.
- [47] Y. Zheng, L. Zhang, X. Xie, and W.-Y. Ma, "Mining interesting locations and travel sequences from gps trajectories," in *Proceedings of the 18th International Conference on World Wide Web*. New York, NY, USA: ACM, 2009, pp. 791–800.
- [48] Y. Zheng, Q. Li, Y. Chen, X. Xie, and W.-Y. Ma, "Understanding mobility based on gps data," in *Proceedings of the 10th International Conference on Ubiquitous Computing*. New York, NY, USA: ACM, 2008, pp. 312–321.
- [49] Y. Zheng, X. Xie, W.-Y. Ma *et al.*, "Geolife: A collaborative social networking service among user, location and trajectory," *IEEE Data Eng. Bull.*, vol. 33, no. 2, pp. 32–39, 2010.